Journal of Hydrology: Regional Studies 61 (2025) 102695

Contents lists available at ScienceDirect

Journal of Hydrology: Regional Studies

journal homepage: www.elsevier.com/locate/ejrh

Seasonal variations and drivers of water quality in semi-arid freshwater lakes: multivariate spatial analysis in Lake Guiers, Senegal

Hikimat Saadi [a,b,d], Djim M.L. Diongue [c], Andrew Ogilvie [d,*], Didier Martin [d], Oumy Tall [b], Johann Bellanger [b], Abib Ndiaye [e], Serigne Faye [a]

[a] *Geology Department, Université Cheikh Anta Diop, Dakar, Fann, Senegal*
[b] *Eau du Sénégal (SEN'EAU), Centre de Hann, route du Front de Terre,BP, Dakar 4945, Senegal*
[c] *École Nationale Supérieure des Mines et de la Géologie, Université Cheikh Anta Diop, BP, Dakar, Fann 5396, Senegal*
[d] *G-EAU, Univ Montpellier, AgroParisTech, BRGM, CIRAD, INRAE, Institut Agro, IRD, Montpellier, France*
[e] *Office du lac de Guiers et des Cours d'eau (OLAC), Senegal*

ARTICLE INFO

Keywords:
West Africa
Freshwater
Water quality
Hydrochemistry
Anthropogenic activities

ABSTRACT

Study region: Lake Guiers, Senegal, West Africa
Study focus: Water quality degradation from agriculture threatens freshwater lakes worldwide. This study investigated the spatiotemporal hydrochemical dynamics of Lake Guiers, which supplies 50 % of Dakar's drinking water, and examined natural and anthropogenic drivers of water mineralization. The approach combined multivariate statistics, hydrogeochemical analysis (Piper, Gibbs), and Water Quality Index (WQI) assessments of samples collected over five seasonal campaigns (2022–2023) as well as hydroclimatic analysis. Seasonal variations and spatial gradients of 22 parameters (physicochemical, major ions, biological, heavy metals) were explored to inform effective freshwater management strategies.
New hydrological insights for the region: Multidisciplinary approach highlights impact of intensified agriculture and inflows on spatiotemporal variations in water quality. WQI values categorized 67–87 % of samples as poor water quality, with conditions worsening during the rainy season. Several parameters including heavy metals, cyanobacteria, chlorophyll-a and turbidity exceeded WHO standards. Temporal variations were influenced by evaporation during the dry season, agricultural discharge, and the combination of runoff and inflow waters during the rainy season. Sediment loaded inflow from the Taouey canal notably leads to greater turbidity and suspended particulate matter in the north of the lake, while runoff and associated mobility of nutrients favour cyanobacteria proliferation during the rainy season. Targeted interventions to reduce pollution sources and continuous monitoring of transitory drainage and runoff in selected hotspots are required to preserve this vital semi-arid freshwater lake.

1. Introduction

Freshwater bodies, especially in semi-arid regions, are crucial to support the multiple water needs of agriculture, industry, domestic

* Corresponding author.
E-mail address: andrew.ogilvie@ird.fr (A. Ogilvie).

https://doi.org/10.1016/j.ejrh.2025.102695
Received 6 June 2025; Received in revised form 2 August 2025; Accepted 4 August 2025
Available online 12 August 2025
2214-5818/

water supply, and ecosystems (Nayek et al., 2017). Unfortunately, many lakes are experiencing pollution through anthropogenic activities in their vicinity, resulting in deteriorating water quality. Polluted water not only threatens human health but also disrupts aquatic ecosystems (Wang et al., 2014; Ouma et al., 2022; Onu et al., 2023; Moto et al., 2024). Anthropogenic activities affecting water quality include agriculture (Ekholm and Mitikka, 2006; Holopainen and Lehikoinen, 2022), livestock management (Li et al., 2022), waste production and disposal (Wang et al., 2014; Bhat et al., 2022; Bangani et al., 2023), and increased sediment runoff or soil erosion due to land use changes (Sani et al., 2024). Furthermore, the construction of dams and limited discharge at outlet dikes may also influence the dynamics of aquatic systems by altering natural flow, heat regimes, sediment transport, and nutrient dynamics (Fantong et al., 2015; Zhang et al., 2022). Natural factors, including variations in climatic parameters such as evaporation, precipitation, and temperature, may also influence lake water quality (Magesh et al., 2013; Woolway et al., 2020), especially in semi-arid regions. Considering the decline in water quality and the scarcity of water resources in semi-arid areas, regular and continuous monitoring of water quality is urgently required to implement protection and preservation measures (Downing et al., 2001; Ayele and Atlabachew, 2021; Danaher et al., 2022).

Physicochemical characteristics such as pH, dissolved oxygen, temperature, turbidity, color, and odor (Guenouche et al., 2024), biological parameters like chlorophyll-*a* and cyanobacteria (Søndergaard et al., 2011), and heavy metals constitute key factors in determining water quality levels, as noted by several researchers (Kazi et al., 2009; Githaiga et al., 2021; Guenouche et al., 2024). These parameters are mostly interrelated and understanding them is critical for effectively managing and improving overall water resource quality (Moeinzadeh et al., 2024).

Water quality assessment involves various appropriate methods to measure specific parameters and contaminants present in water (Moeinzadeh et al., 2024). In Asia, lakes in Panchkula (India) face challenges from agricultural runoff and severe soil erosion. To address these issues, methods like Pearson's correlation coefficient analysis, Principal Component Analysis (PCA), and Hierarchical Cluster Analysis (HCA) have been applied to identify pollution sources and characterize water quality (Vasistha and Ganguly, 2024). Dal Lake (India) and Lake Chagan (China) have experienced water quality degradation due to economic growth and urbanization, resulting in increased industrial effluents, domestic discharges, and agricultural runoff (Liu et al., 2019; Saleem et al., 2015). Hydrochemical investigations are primarily tools for detecting degradation trends and informing sustainable water management practices. Similarly, Lake Daihai, in a semi-arid basin (Northern China), has experienced a reduction in surface area and biodiversity, alongside water quality degradation caused by excessive fertilizer and pesticide use, as well as improper domestic wastewater discharge (Ren et al., 2022).

Furthermore, Water Quality Indices (WQIs) are widely employed across various regions to assess and inform on water quality based on specific parameters (Chidiac et al., 2023; González et al., 2024; Guenouche et al., 2024; Sishu et al., 2024). In Ethiopia, Lake Tana, the country's largest freshwater reservoir, is impacted by leaching runoff from agricultural lands, urban discharges from 17 watersheds, and sedimentation from cultivated fields (Sishu et al., 2024). WQI was employed to evaluate pollution levels, complemented by geospatial analysis, hierarchical classification, and PCA to identify probable pollutant sources.

The current study focuses on Lake Guiers, which constitutes the primary freshwater reserve in Senegal. Located on the left bank of the Senegal River, it provides important ecosystem services to thousands of inhabitants and supports crucial livelihoods such as fishing, irrigation, livestock, and ecotourism. Additionally, since the early 1970s, the lake has served as the main source (50 %) of drinking water for the capital city (Dakar) through a piped transfer system (Kamara et al., 2021). During the last few decades, available studies on this hydraulic system's water quality (Cogels et al., 1997, 2001) have highlighted profound changes in the chemical composition and dynamic changes of the water in the lake basin, inferred by the construction of the Diama (downstream) and Manantali (upstream) dams. In addition, the region has experienced substantial agricultural growth driven by increased interest in its freshwater and fertile land (Bruckmann et al., 2025, Ogilvie et al., 2025). In recent years, the lake has been subject to increased wastewater discharge from agro-industries, with potentially high nutrients, heavy metals, and pesticides (including other prohibited compounds) contents, as evidenced by various investigations (OLAC, 2013, 2016; Niang et al., 2017; Bah et al., 2022). Solid waste dumped at various places around the lake could also contribute to pollution levels.

Given the strategic role of Lake Guiers in terms of food production and water security, it is crucial to comprehensively understand the factors affecting its quality. With regard to this challenge, some studies have focused their investigations on the overall trophic status and sedimentation (e.g., Varis and Fraboulet-Jussila, 2002; Kâ et al., 2006; Sane et al., 2015; Diédhiou et al., 2019) without exploring the sources and spatio-temporal variation of solutes. To address this research gap, it is important to consider natural and anthropic processes occurring with a special emphasis on their spatio-temporal variability.

This study therefore aims to identify the primary drivers of water mineralization in Lake Guiers, focusing on the factors involved, and how seasonal variations affect them. Our specific objective is to discriminate key processes influencing water mineralization, and to differentiate natural and human-induced impacts through hydrochemical and statistical analyses that will inform on efficient management and contribute to food and water security.

2. Materials and methods

2.1. Study area description

Lake Guiers is located between latitudes 15°56' and 16°35' North and longitudes 15°47' and 16°15' West, at the heart of the Ferlo hydrological catchment (46,000 km^2). The soil in the basin is predominantly composed of tropical ferruginous soils, followed by lithosols and subarid red-brown soils (Fig. 1a). Hydrologically, this basin is nearly inactive due to low rainfall in this region. However, Lake Guiers is fed by the Senegal River through the Taouey Canal and can discharge to the Lower Ferlo via the Keur Momar Sarr dam bridge. The lake extends approximately 50 km in length, reaches up to 7 km in width, and has a maximum depth of 4 m (Cogels et al., 2001). The lake area covers 350 km^2 with a volume of 450 million m^3 at a water level of 1.5 m IGN, which can increase to 750 million m^3 at a 2.5 m water stage after floods (Fig. 1b).

The region's climate, situated in the Sahelian zone, is semi-arid, characterized by a short rainy season lasting 3–4 months between

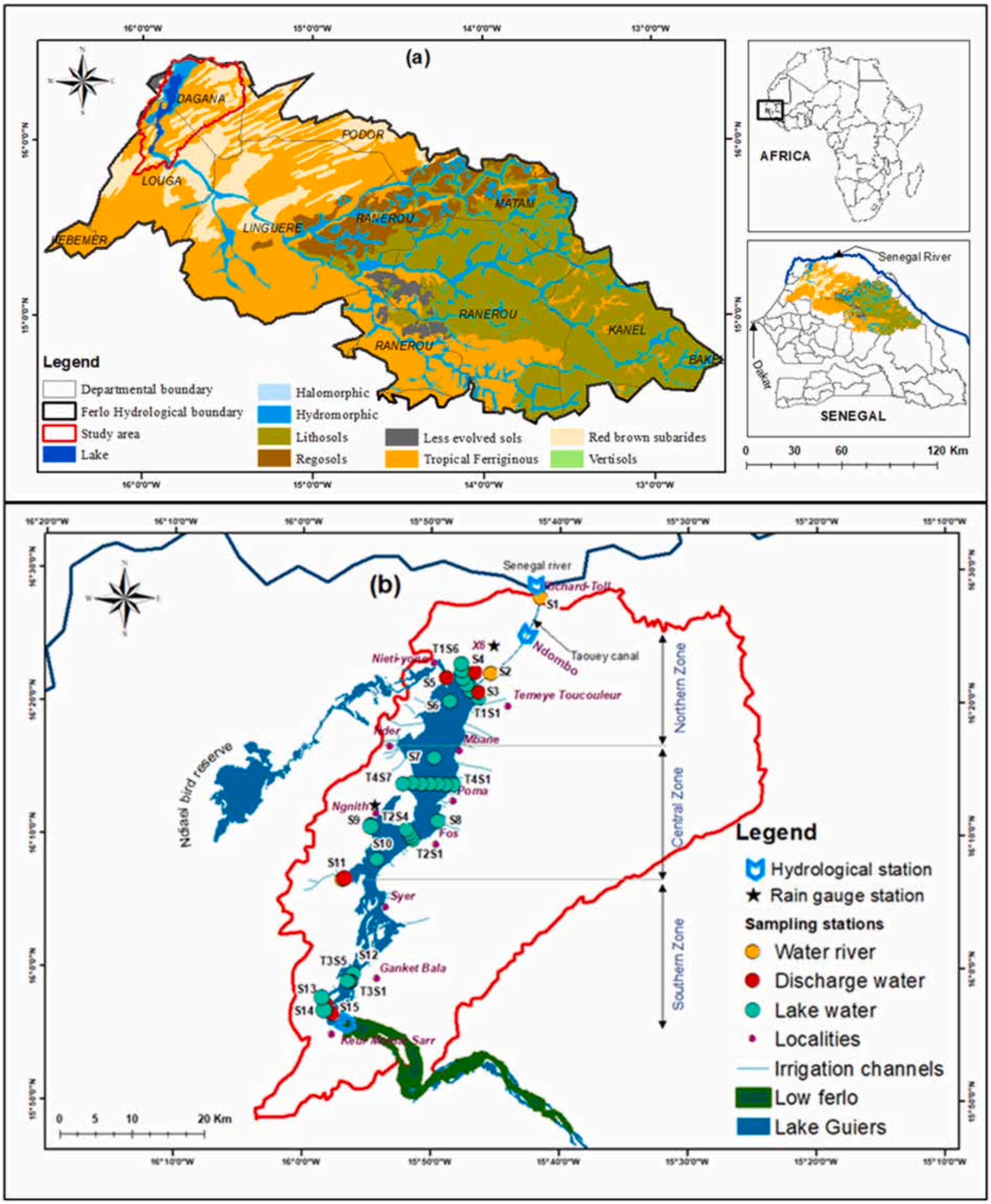

Fig. 1. Location of the study area showing the (a) soil types in the Ferlo basin, (b) sampling points around Lake Guiers.

July and October, followed by a long dry season. Precipitation is relatively low and extremely variable over the years, with an annual average of 200–250 mm over the last 30 years (Ndiaye et al., 2024). Runoff is low in the region, and consequently, the lake inflow is mainly derived from the Senegal River via the Taouey Canal. The average annual temperature is high, reaching 27.8°C (data from 1960 to 2020 from weather stations located near the lake in Saint-Louis), and potential evapotranspiration (ET_0) exceeds 2500 mm per year. The dry season is primarily characterized by northeast winds (known locally as Harmattan) blowing along the lake's major axis, while the rainy season is marked by northwest winds (maritime trade winds) (Sane et al., 2015).

2.2. Hydroclimatic data

The hydroclimatic data employed in this study consists of climatic parameters (temperature, rainfall, evaporation) and limnimetric measurements on Lake Guiers (see Fig. 1b). Temperature and evaporation data were acquired from field monitoring carried out by the Compagnie Sucrière Sénégalaise (CSS) on the left bank of the Taouey canal (station X6). Lake evaporation was estimated from pan evaporation values converted using a pan transposition coefficient of 0.6, based on previous studies (Cogels et al., 1997).

Rainfall data were measured by SENEAU at the Ngnith station, located at the drinking water treatment plant. Local runoff from these rainfall events was estimated here based on the catchment area (354 km^2) and a runoff coefficient (10 %) derived from previous water balance modelling (Cogels et al., 1997; Cogels and Gac, 1981). Water level monitoring is implemented by the Office des Lacs et Cours d'Eau (OLAC) at several locations, however time series do not all cover the entire study period. Here limnimetric data from the Richard-Toll dam bridge which monitors inflows from the Senegal River through the Taouey canal and from a limnimetric stage ladder at the intake to the Ngnith drinking water treatment plant were used. The monthly average flow entering the Taouey canal over the period 2010–2021 is presented in Fig. 2 to illustrate the amplitude and seasonal variability of water inflows.

2.3. Water quality sampling and measurement procedures

2.3.1. Selection of water quality parameters

The water quality parameters measured in this study include physicochemical, ionic, phytoplanktonic, and heavy metal indicators (Table 1). Their selection was guided by previous studies carried out on Lake Guiers (Cogels et al., 1993; Diédhiou et al., 2019) as well the relevance of these parameters based on the dominant activities observed around the lake which include agriculture, livestock and drinking water treatment. Furthermore, the recommendations of the World Health Organization (WHO, 2017) for water quality assessments were integrated to include sanitary, environmental, and operational standards.

Water temperature constitutes a critical limiting factor for aquatic organisms, including fish populations (Kalny et al., 2017), and influences numerous biochemical processes in the lake ecosystem. pH also affects the biological and chemical equilibria of freshwater lakes while dissolved Oxygen (DO) is a key indicator of aquatic ecosystem health. A low level of DO in water is a sign of contamination and is an important factor in determining water quality, pollution control, and treatment processes (Crossman et al., 2019). Turbidity, particulate matter (SPM), organic matter (OM), and total organic carbon (TOC) provide information on the sedimentary and organic load of the system, linked to erosion, runoff, and agricultural or urban discharges (Palviainen et al., 2016; Sane et al., 2015). Electrical conductivity (EC) reflects the degree of water mineralization, influenced by agricultural inputs and salinization. Analysis of major ions (Na^+, Ca^{2+}, Mg^{2+}, K^+, Cl^-, SO_4^{2-}, HCO_3^-, NO_3^-) help understand the presence of anthropogenic inputs (fertilizers, drainage) and the geochemical origin of dissolved salts, as well as processes such as ion exchange and dissolution of surrounding geological formations (Niang et al., 2022; Saleem et al., 2015).

Some physicochemical and ionic parameters are already monitored daily at SENEAU/SONES drinking water intake stations, especially at Ngnith (see Fig. 1b), but no comprehensive spatial assessment had previously been conducted over the entire lake. This study also integrates additional parameters indicative of algal blooms, such as chlorophyll-a (Chl-a), previously used to assess eutrophication risk (Diédhiou et al., 2019), and cyanobacteria, which are potentially toxic and problematic for public health and water treatment systems. Heavy metals were also measured to identify both natural and anthropogenic impacts (Sishu et al., 2024; Tokatlı et al., 2024; Yuksel et al., 2021).

Water quality was evaluated based mainly on thresholds defined by WHO guidelines (WHO, 2017). For parameters not covered by WHO, values from United States Environmental Protection Agency (USEPA, 2022), Senegalese national standards (Institut Sénégalais

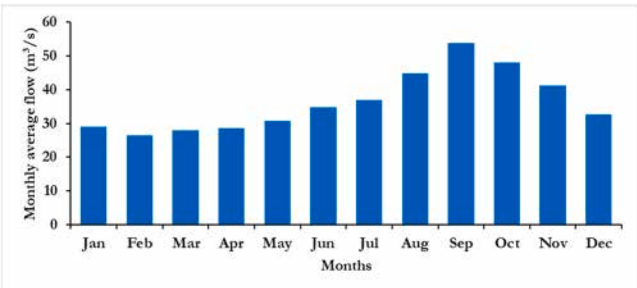

Fig. 2. Monthly average inflow into the Taouey canal (2010–2021).

Table 1
Characteristics of the sampling campaigns on Lake Guiers.

Sampling period	Sampling stations	Season & temp (°C)	Evaporation (mm/day)	Rainfall (mm)	Level lake average (m IGN)	Parameters			
						Physico-chemical	Ionic	Phytoplankton	Heavy metal
March 28 to April 1 2022	N = 16	Dry hot (26.7)	5.3	0	2.20	X	X	X	
May 6–10, 2022	N = 15	Dry hot (30)	5.5	0	2.17	X	X	X	
August 11–19, 2022	N = 31	Rainy (30.2)	3.7	1.0	2.35	X	X	X	
October 11–17, 2022	N = 38	Rainy (31.5)	4.0	4.8	2.69	X	X	X	
February 17–21, 2023	N = 38	Dry hot (27.4)	5.5	0	2.18	X	X	X	X

de Normalisation ISN, 2001), and Chinese standards (GB/T 5749–2006, cited in Jiang et al., 2022) were used, as summarized in Table 2.

2.3.2. Collection of water samples

To understand the dynamics of water quality in Lake Guiers throughout the year, we conducted a series of measurements at multiple locations. Water samples were collected over five months, specifically during the dry season (March and May) when the lake level is at its lowest; at the beginning of the rainy season (August); at the end of the rainy season (October) when the water level reaches its maximum; and when the lake waters begin to recede (February) (Table 1). Sampling sites were carefully selected based on proximity to potential pollution sources identified around Lake Guiers during field surveys, accessibility and hydrographic distribution.

Sampling points were primarily located at the Taouey Canal (2 sites), at agro-industrial discharge points (6) into the lake, at the outlets of major irrigation canals (3), and in zones in the vicinity of villages (3) to capture anthropogenic influence (Fig. 1b). Additionally, four transects were selected to provide an overview of water quality along the north-south axis of the lake (Table S1 in the supplementary materials). Samples for chemical analysis were stored in 0.3-liter polyethylene bottles (for ions) and 1-liter bottles (for other parameters). The bottles were carefully rinsed three times before use and stored in a cooler at 4°C until laboratory analysis.

2.3.3. Analysis of water samples

The following physicochemical parameters were recorded in situ using an Aqua Troll 500 multiparameter device (In-Situ Inc, USA) which includes temperature, pH, dissolved oxygen (DO), electrical conductivity (EC), and turbidity probes. Phytoplankton parameters, including cyanobacteria and chlorophyll-a, were measured using a Hydrolab - DS5 probe (OTT HydroMet GmbH, Germany). The probes were calibrated and standardized prior to field measurements.

The ionic parameters and heavy metals were analyzed at the UCAD hydrochemistry laboratory. The ions were quantified by ion chromatography using an AQUION-DIONEX system. Ion exchange processes were performed using AS14 A-AERS 500 columns for anions (Cl^-, NO_3^-, SO_4^{2-}) and CS12 A-CERS 500 columns for cations (Na^+, K^+, Mg^{2+}, Ca^{2+}). HCO_3^- ions were determined by titration with sulfuric acid solution. The accuracy of the chemical analyses was verified by ion balance, with values ranging between 5 % and 8 %, thus confirming the reliability of the data.

Heavy metals (Fe, Mn, Cu, and Zn) were analyzed by atomic absorption spectrometry using a Thermo ICE 3000 spectrometer. Other parameters, such as particulate matter (SPM), organic matter (OM by UV absorbance at 254 nm), and total organic carbon (TOC), were measured photometrically using a DR 6000 spectrophotometer. TOC analysis involved colorimetric oxidation in a reactor (DRB200) at 180°C for 2 h, followed by measurement on the DR 6000 at the central laboratory of the Senegalese Water Company (SEN'EAU) (Table S2).

2.4. Land use data

Land use data for the study area was derived from global land use and land cover datasets made available online by the European Space Agency (ESA). The CCI-LC maps were produced through the processing of full archives from MERIS (300 m), SPOT-Vegetation (1 km), PROBA-V (1 km), and AVHRR (1 km) sensors, resulting in 28 annual land cover classifications from 1992 to 2019. To analyze long-term changes, we used ESA's Land Cover (CCI-LC) products at 300-meter resolution from 1992 and Sentinel-2-based land cover data at 10-meter resolution from 2020. The images were then processed using QGIS software to perform a supervised classification of land uses and compute the surface area of each class.

Table 2
Summary statistics for the water quality parameters collected in March, May, August, October and February in Lake Guiers.

			Shapiro–Wilk test					Kruskal–Wallis test by month		Kruskal–Wallis test by sites	
Variables/Month	Units	Guideline thresholds	March−2022	May−2022	Aug-2022	Oct−2022	Feb-2023	H	*p*	H	*p*
Temp	°**C**		0,0542	**0,0130**	0,6388	0,4021	0,0532	52,8800	**0,0000**	12,8371	0,9998
pH		6.5–8.5*	0,5330	0,3583	0,0568	**0,0000**	0,0171	34,4333	**0,0000**	33,9720	0,5176
EC	**µs/cm**	≤ 1500*	**0,0159**	0,3032	**0,0000**	**0,0001**	**0,0008**	3,3797	0,1845	51,4427	**0,0360**
DO	**mg/L**	< 2**	0,0540	0,4050	0,1171	**0,0000**	**0,0002**	31,7012	**0,0000**	36,5761	0,3955
Turb	**NTU**	5*	**0,0002**	0,4806	0,2235	**0,0000**	**0,0016**	8,5792	**0,0137**	22,3093	0,9525
Chl-*a*	**µg/L**	12**	**0,0049**	**0,0035**	**0,0021**	**0,0002**	**0,0009**	42,1076	**0,0000**	20,3343	0,9773
Cyano	**cells/mL**	20000*	0,0888	**0,0079**	**0,0367**	**0,0005**	**0,0000**	40,5851	**0,0000**	17,8882	0,9927
SPM	**mg/L**	≤ 40***	**0,0285**	**0,0498**	**0,0025**	**0,0000**	**0,0001**	7,4649	**0,0239**	32,6288	0,5831
OM	**UV 250 (m^{-1})**	5*	0,3976	**0,0000**		**0,0000**	**0,0000**	14,9539	**0,0006**	29,5918	0,7265
TOC	**mg/L**	5***	**0,0000**		**0,0001**	**0,0040**	**0,0005**	2,1787	0,3364	39,9951	0,2580
Ca^{2+}	**mg/L**	≤ 100*	**0,0000**	0,2898	**0,0000**	**0,0000**	**0,0000**	7,3165	**0,0258**	52,0680	**0,0317**
Mg^{2+}	**mg/L**	≤ 50*	0,0666	0,4764	**0,0029**	0,1208	**0,0044**	2,2187	0,3298	46,7091	0,0891
Na^{+}	**mg/L**	≤ 200*	0,7443	0,2661	0,0581	**0,0000**	**0,0000**	1,7724	0,4122	61,9123	**0,0033**
K^{+}	**mg/L**	10 – 15*	0,3336	0,0643	**0,0034**	**0,0006**	**0,0014**	2,5374	**0,0433**	60,1244	**0,0052**
$HCO3^{-}$	**mg/L**	≤ 200*	0,7456	0,2490	0,2304	**0,0028**	**0,0015**	1,2256	0,5418	63,3776	**0,0023**
Cl^{-}	**mg/L**	≤ 250*	0,3506	0,3477	**0,0006**	**0,0000**	**0,0000**	1,8732	0,3920	62,9677	**0,0026**
SO_4^{2-}	**mg/L**	≤ 250*	**0,0000**	0,1286	**0,0000**	**0,0000**	**0,0000**	9,3983	**0,0091**	53,3660	0,0242
$NO3^{-}$	**mg/L**	≤ 50*	0,0711	0,0756	**0,0001**	**0,0000**	**0,0001**	2,5903	0,2739	60,4561	**0,0048**

Bold values in this table are Shapiro-Wilk and Kruskal-Wallis test *p-values* that are inferior to 0.05,
* WHO standards,
** USEPA standards,
*** Other standards: TOC (Chinese national standard for drinking water quality (GB/T 5749–2006) and SPM: Senegalese standard NS 05–061.

2.5. Statistical analysis and visualization

Water quality data were analyzed using conventional hydrogeochemical tools such as PIPER (Piper, 1944) and CHADHA (Chadha, 1999) diagrams in conjunction with multivariate statistical methods. The Shapiro-Wilk (SW) data normality test was used to check if water quality parameters conformed to statistical normal distribution (Sani et al., 2024). The Kruskal-Wallis (KW) test was used to detect significant seasonal differences among the different water quality parameters (Woldeab et al., 2019). *p-values* of the Shapiro-Wilk test below 0.05 ($p < 0.05$) indicate that data are not normally distributed and $p < 0.05$ for the Kruskal-Wallis test indicates a significant seasonal difference between dry and rainy season data for each parameter.

Statistical methods combined correlation matrix, Principal Component Analysis (PCA), and hierarchical clustering analysis (HCA), which are widely used in water quality assessments (Kazi et al., 2009; Gaury et al., 2018; Liu et al., 2019; Yuksel et al., 2021; Karadeniz et al., 2024). Water quality parameters were first subjected to Pearson correlation analysis with Python programming. This step aimed to examine the interrelationships between the analyzed parameters (pollutants/contaminants) and their potential sources in the lake. Parameters with correlation coefficients ($|r|$) > 0.7, $0.7 > |r| > 0.5$, and $|r| < 0.5$ were considered strong, moderate, and weak, respectively (e.g. Li et al., 2024). The absolute value of their correlation coefficients ($|r|$), as r can also be negative.

PCA and HCA were performed in R to identify pollution sources and sample groupings. Prior to PCA application, all water quality parameters were standardized (z-score normalization) to ensure variables with different units and scales contributed equally to the analysis, following standard multivariate statistical practices. The rationale for using PCA was to transform the correlated water quality variables into uncorrelated components that capture the maximum variance in the dataset, thereby revealing underlying pollution patterns and sources that may not be apparent from individual parameter analysis. Principal components with eigenvalues > 1 (Kaiser's rule) were retained for interpretation, as these components explain more variance than any single original variable (Kaiser, 1960). Variable loadings > 0.75, 0.50–0.75, and < 0.50 were considered high, moderate, and low contributions to each principal component, respectively (Egbueri and Mgbenu, 2020).

HCA was subsequently applied using Ward's linkage method with Euclidean distance to group samples with similar water quality and contamination profiles. This approach allows for the identification of distinct water quality zones within the study area, therefore facilitating targeted management strategies.

The spatial distribution of water parameters was mapped in a Geographic Information System (GIS) and interpolated using Inverse Distance Weighting (IDW), a method suitable when analyzing data with no outliers.

2.6. Water quality evaluation

2.6.1. Water Quality Index (WQI)

Water quality was evaluated using the Water Quality Index (WQI), a widely recognized approach that provides a comprehensive evaluation of overall water quality based on the influence of individual parameters (González et al., 2024; Guenouche et al., 2024; Sishu et al., 2024; Benam-Beltoungou et al., 2025). The weight of various water quality parameters is assumed to be inversely proportional to the recommended standards for each parameter (e.g., Diongue et al., 2022).

The calculation procedure involved three stages. First, each of the 13 parameters (pH, DO, EC, Turbidity, Chl-a, Ca^{2+}, Mg^{2+}, Na^{+}, K^{+}, HCO_3^-, Cl^-, SO_4^{2-}, and NO_3^-) selected based on their public health significance, was assigned a weight (w_i) on a scale of 1–5 based on its perceived health effects and importance in drinking water quality (Nair et al., 2020; Xiao et al., 2020; Guenouche et al., 2024).

Second, the relative weight (W_i) was computed using Eq. 1:

$$W_i = \frac{w_i}{\sum_{1}^{n} w_i} \quad (1)$$

Where w_i is the weight of an individual parameter, and n represents the total parameter count. The computed values for each parameter's relative weight (W_i) are provided in supplementary materials (Table S3).

Third, the quality rating scale (q_i) for each parameter was calculated by dividing its concentration by its respective WHO standard and multiplying the result by 100:

$$q_i = \frac{C_i}{S_i} * 100 \quad (2)$$

Where C_i is the concentration of each chemical parameter in milligrams per liter, and S_i is the World Health Organization (WHO) standard for each chemical parameter in milligrams per liter (WHO, 2014).

In the final step, the sub-index (SI_i) for each parameter was calculated, followed by the overall WQI computation:

$$SI_i = W_i * q_i \quad (3)$$

$$WQI = \sum SI_i \quad (4)$$

The resulting WQI values were classified according to established categories (Guenouche et al., 2024): excellent water ($WQI < 50$), good water (50−100), poor water (100−200), very poor water (200−300), and water unsuitable for drinking purposes ($WQI > 300$).

2.6.2. Suitability for irrigation

Excessive salinity in irrigation water can cause soil salinization, whereas high Na concentrations can cause soil alkalinization, compaction, and reduced permeability (Gaury et al., 2018; Ren et al., 2022). The Soluble Sodium Percentage (SSP), expressed as Na%, is a key criterion for classifying irrigation water quality. It is calculated using the following equation:

$$Na\% = [(Na^{+} + k^{+}) / (Ca^{2+} + Mg^{2+} + Na^{+} + k^{+})] \ x \ 100 \quad (5)$$

The calculated SSP values were plotted against electrical conductivity (EC) on the Wilcox diagram (Wilcox, 1955) to classify lake water suitability for irrigation purposes.

3. Results

3.1. Seasonal dynamics of climate and hydraulic management between 2022 and 2023

Analysis of hydroclimatic variations helped define the conditions specific to each of the five field campaigns (C1 to C5), as highlighted in Fig. 3 and Fig. 4, and summarized in Table 1. Fig. 3 illustrates variations in air temperature, precipitation, and evaporation in the study area at a daily time step from January 2022 to February 2023. The average annual air temperature was 28.0°C, with a bimodal pattern: a first peak reaching approximately 35°C in May-June, a second peak around 30°C in September-October, and a minimum of approximately 19.5°C in February. Evaporation followed a similar trend, with higher rates (5–9 mm/day) during the dry season, particularly between March and May, coinciding with rising temperatures. Lower values (3–4 mm/day) are observed during the rainy season, due to the higher humidity levels.

During this period, 38 rainy days were recorded, mainly concentrated between August 6 and October 20, 2022, indicating a late start to the rainy season (typically July-October). The average daily rainfall during precipitation events was extremely low (approximately 1 mm), and only four days exceeded 20 mm. An intense rainfall event (110.8 mm) was recorded on August 25, but occurred after the C3 water quality monitoring campaign. Runoff from these events is estimated to reach a total of 11 Mm^3, with a peak of 3.9 Mm^3 during the August 25 storm. Storm hydrographs are not available for the lake but assuming a 1-day propagation time and homogenous rainfall across the 354 km^2 catchment, this storm would equate to runoff of 45 m^3/s over 24 h. Average inflow through the Taouey canal ranges between 27 and 54 m^3/s, reaching 45 m^3/s in August and a peak of 54 m^3/s in September. These results highlight the limited contribution from local runoff compared to the Senegal River. Nevertheless, continuous monitoring of water quality levels around the lake would help further determine the impact of local runoff events on pollutant flushing.

Fig. 4 illustrates the hydrological dynamics of Lake Guiers based on the limnimetric measurements at the Ngnith station and the local rainfall data. The water levels at Ngnith averaged 2.27 m IGN throughout the study period, with a minimum of 1.97 m and a maximum of 2.69 m, depicting a clear annual dynamic. Water levels remained relatively stable between January and July 2022 around 2.2 m. Water levels rise substantially from mid-July and reach a peak in mid-October, before declining in November-December and stabilizing again in January-February 2023. Fig. 4 also highlights how the lake levels mirror the limnimetric changes in the Senegal River and Taouey canal. A small rise is observed from the runoff after the August 25 event, but the lake water level dynamics are primarily driven by inflow from the Taouey canal. The Lake Guiers water levels are regulated through the Richard-Toll (upstream) and Keur Momar Sarr (downstream) weirs. When the Senegal River level exceeds that of the lake, both gates are opened to facilitate inflow and the filling of the lake. Conversely, between mid-October and mid-February, as river levels decrease, the downstream gate is closed to prevent backflow, while the upstream gate typically remains open (Bader, 2015).

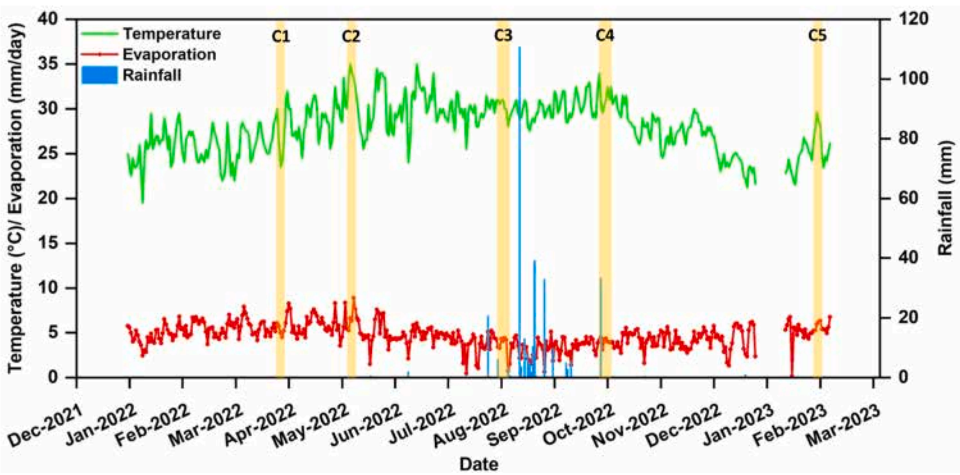

Fig. 3. Daily variation of air temperature, evaporation, and rainfall from January 2022 to February 2023.

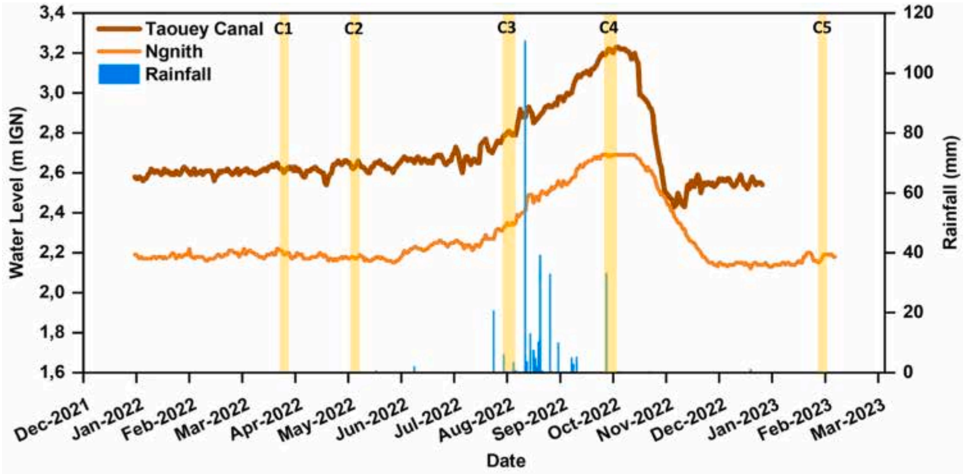

Fig. 4. Daily variation of rainfall and Lake Guiers water level at Ngnith station and in Taouey canal from January 2022 to February 2023.

3.2. Land use dynamics around Lake Guiers basin

The analysis of land use dynamics highlights significant transformations in land cover types around Lake Guiers between 1992 and 2020 (Fig. 5). Irrigated agriculture increased by 50 %, expanding from 20,560 ha in 1992–30,750 ha in 2020, reflecting shifts in agricultural practices and intensification. In contrast, rainfed agriculture showed a decreasing trend of 16.02 %, from 3080 ha to 2590 ha over the same period. Aquatic vegetation exhibited a slight increase of 6.18 %, from 5970 ha to 6340 ha. Urban areas expanded moderately, rising by 11.35 %, from 282 ha to 314 ha, while barren lands significantly decreased.

These land use changes indicate increasing pressure on water resources due to agricultural expansion and urbanization. The conversion of over 10,000 ha to irrigated agriculture suggests a shift towards intensified farming systems, which can have implications for water demand and pollution levels (Englert et al., 2015; Sani et al., 2024).

3.3. Spatial and temporal variation of water quality

The statistical information on water quality parameters is summarized in Table 2. According to the Kruskal-Wallis analysis, there are statistical differences between months for the following parameters: temperature, pH, turbidity, Chl-a, cyanobacteria, SPM, OM, Mg^{2+}, and SO_4^{2-}, and secondarily between sites for the parameters EC, Ca^{2+}, Na^+, K^+, HCO_3^-, Cl^-, and NO_3^-. All measured parameters fall within WHO and USEPA standards, except for pH at a few sites and the following parameters: turbidity, SPM, OM, cyanobacteria, Chl-

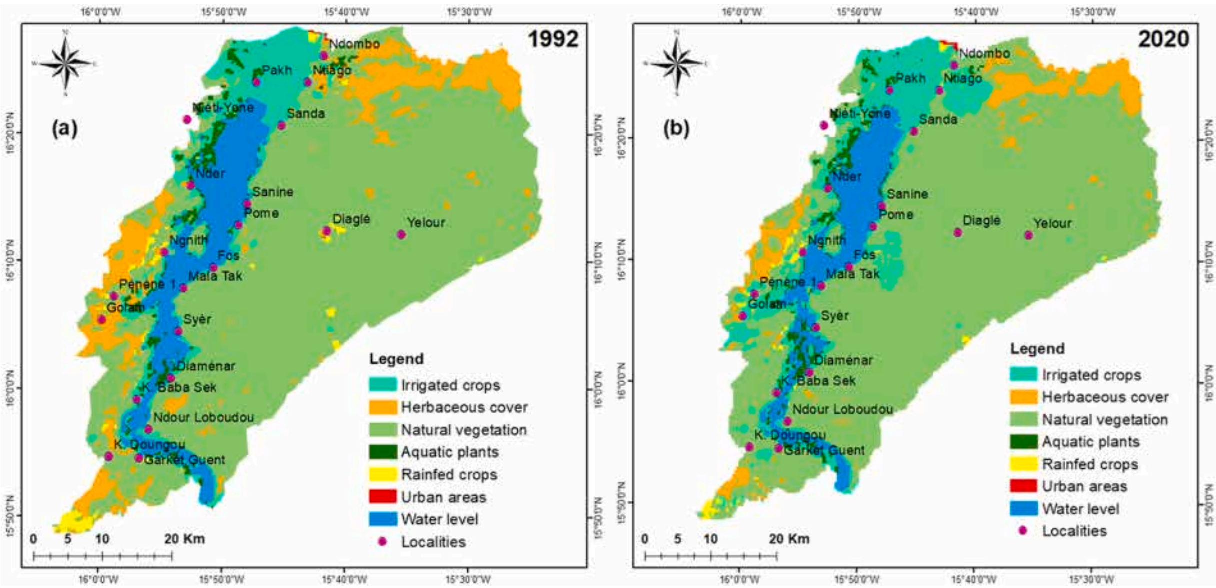

Fig. 5. Spatial dynamics of Land Use around Lake Guiers (1992–2020).

a, and TOC.

Spatially (Fig. 6), the highest concentrations of turbidity, SPM, and OM are recorded in the northern part of the lake. Similarly, parameters controlling water mineralization, including EC, Ca^{2+}, Mg^{2+}, Na^{+}, K^{+}, Cl^{-}, SO_4^{2-}, NO_3^{-}, and HCO_3^{-}, are particularly elevated at sites S4, T1S6, and S15.

The boxplot analysis (Fig. 7) reveals distinct seasonal temperature patterns in Lake Guiers. The mean water temperature across all sampling periods was 27.9°C, with statistically significant inter-monthly variations ($p < 0.001$). Maximum temperatures were observed during the rainy season (August-October), reaching an average of 30.4°C, while minimum temperatures occurred in February during the Harmattan period (average 23.3°C), representing a seasonal amplitude of approximately 7°C. This thermal regime is primarily driven by regional climatic conditions, with water temperatures closely tracking ambient air temperature patterns, which ranged between 30.2 °C and 31.5 °C during the study period.

The pH measurements across the lake exhibited a mean value of 7.6, with statistically significant monthly variations ($p < 0.001$). Notably, pH values displayed a seasonal pattern, with distinctly acidic conditions (4.6–5.43) recorded in October at the end of the rainy season. Conversely, February sampling revealed alkaline conditions, with maximum values reaching 9.1. This pH range (4.6–9.1) demonstrates the dynamic nature of the lake's acid-base equilibrium, which is fundamental in regulating numerous biogeochemical processes, including nutrient availability, metal solubility, and aquatic organism metabolism (Matta et al., 2017). While most sampling locations maintained pH values, several monitoring sites (e.g., S5, S8, T4S1, and T3S1) exhibited concerning elevated values exceeding 8.5. The concentrations of dissolved oxygen (DO) range from 2.03 to 9.20 mg/l and show significant variations across months ($p < 0.001$). The lowest levels are observed in October (average of 6.29 mg/l), while the highest levels are recorded in March and February (> 8 mg/l), indicating better oxygenation of the lake. DO levels fluctuate close to the minimum requirement of 2 mg/l (USEPA, 2022).

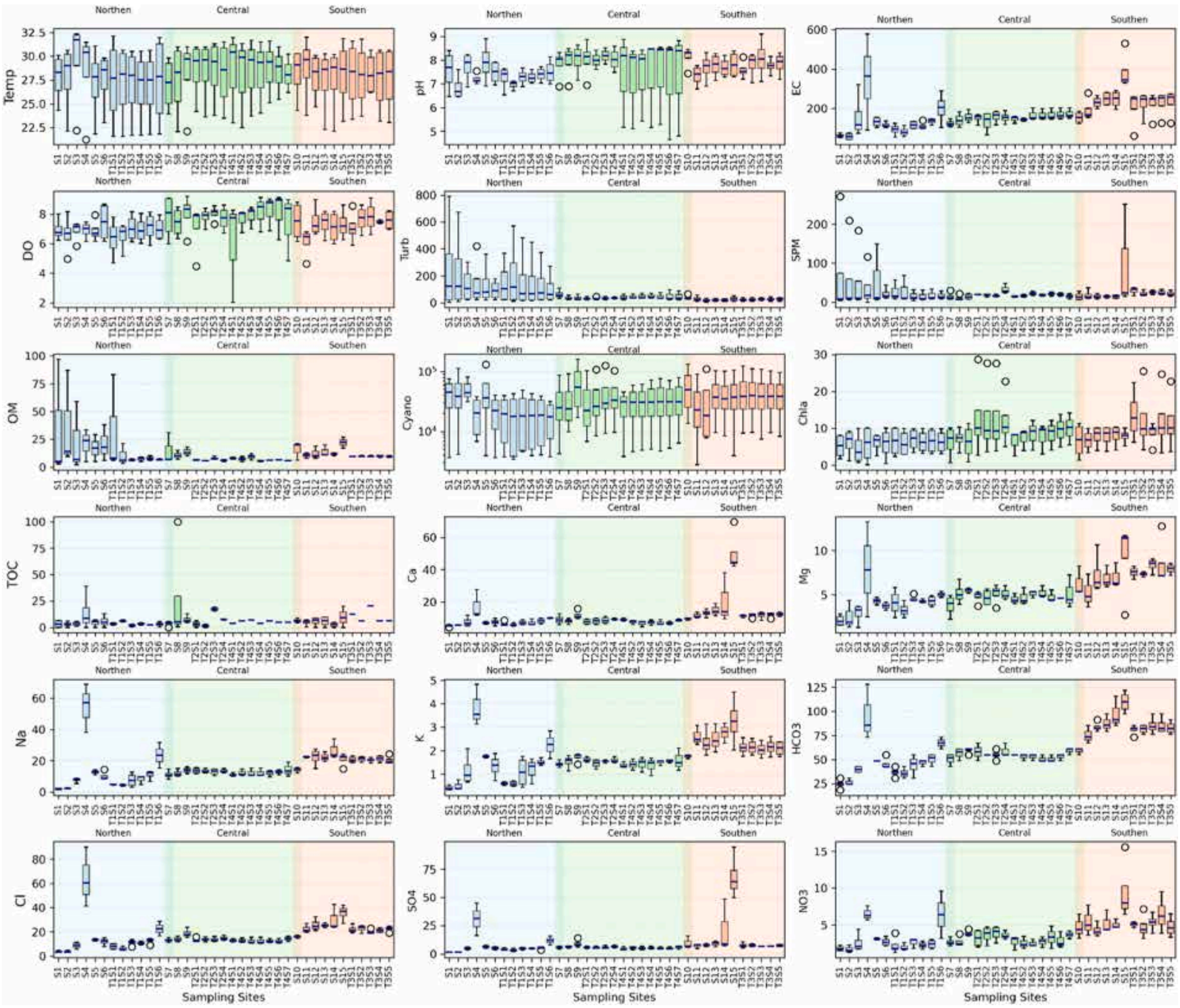

Fig. 6. Boxplots of water quality parameters at different locations of Lake Guiers across the sampling periods.

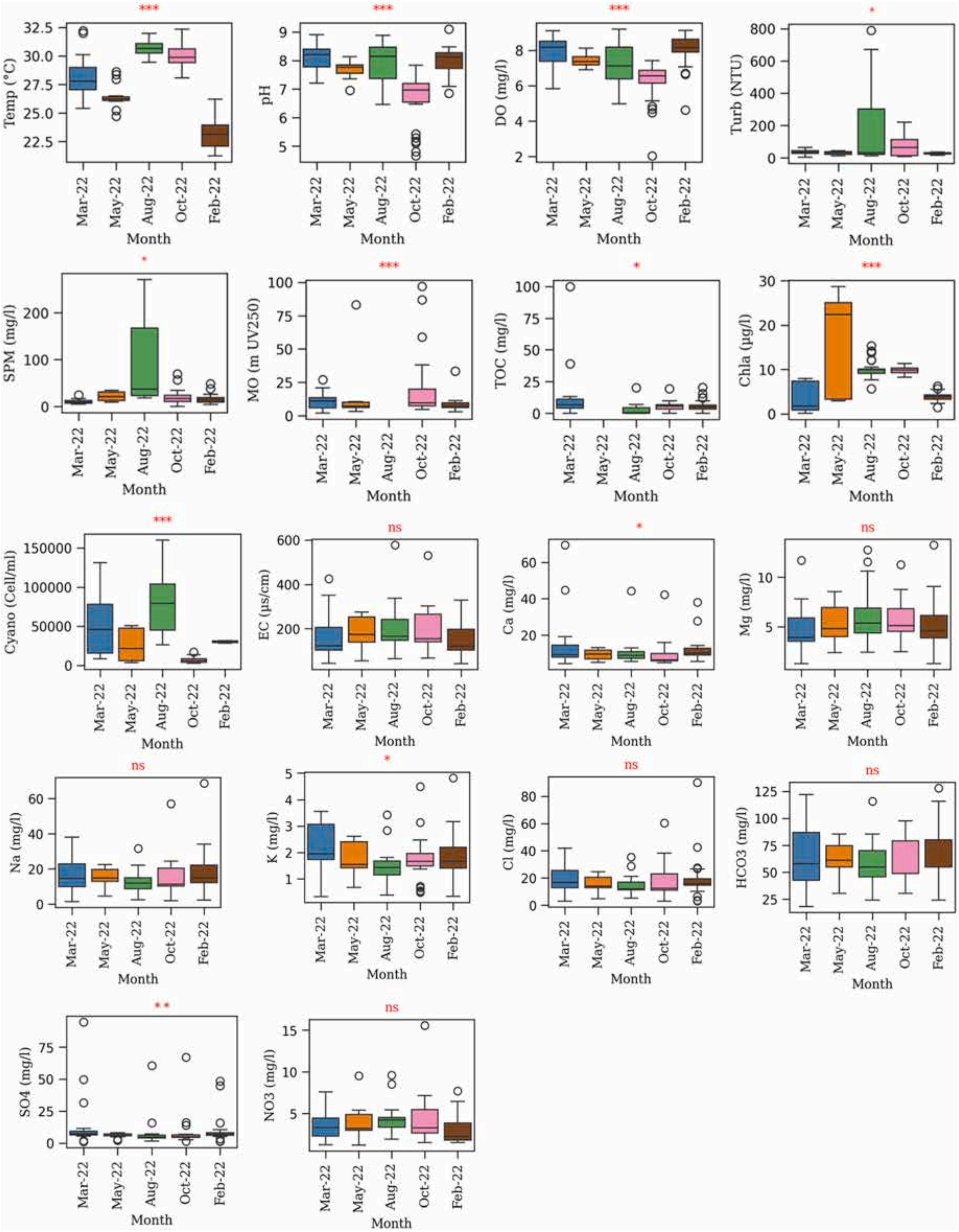

Fig. 7. Boxplots of water quality parameters across months at the Lake Guiers (ns: P > 0.05; *: P ≤ 0.05; **: P ≤ 0.01 and ***: P ≤ 0.001).

Turbidity and SPM also vary across months ($p < 0.05$), with maximum levels of 800 NTU and 250 mg/l, respectively, in August. OM levels fluctuate between 2.0 UV-254 (m^{-1}) in March and 97 UV-254 (m^{-1}) in October ($p < 0.001$). TOC concentrations ranged from 0 to 100 mg/l, with an average of 6.71 mg/l, exceeding the drinking water quality standard of 5 mg/l (Jiang et al., 2022) but remaining within the typical range for surface waters (2–12 mg/l) (Visco et al., 2005). Statistical analyses ($p > 0.05$) show no significant spatio-temporal variations across the lake. However, localized hotspots were identified at specific sites: S4 (40 mg/l, in March 2022), associated with fertilizer runoff, S8 (100 mg/l), near urban discharge, and S15 (20 mg/l in August 2022), close to effluents from drinking water treatment plants.

Chlorophyll-*a* and cyanobacteria concentrations vary significantly across months ($p < 0.001$). The highest Chl-a values are recorded in May (3–28.7 μg/l), while the lowest are observed in February (1.4–6.3 μg/l). As for cyanobacteria, high concentrations are recorded in March and May (hot season) as well as in August (rainy season). The electrical conductivity of the lake water does not vary over the months but rather across the sites, with high values reaching 578 μS/cm in the northern part of the lake. The average concentration of cations and anions varies with the following order of abundance: Na^{+} (14.9 mg/l) > Ca^{2+} (10.8 mg/l) > Mg^{2+} (5.4 mg/l) > K^{+} (1.7 mg/l) and HCO_3^- (61.1 mg/l) > Cl^- (16.9 mg/l) > SO_4^{2-} (8.8 mg/l) > NO_3^- (3.8 mg/l), respectively. Ca^{2+} and Mg^{2+} are essential cations in water, influencing water hardness. Ca^{2+}, K^{+}, and SO_4^{2-} show significant variations between months ($p < 0.05$) with relatively low concentrations throughout the year. In contrast, Mg^{2+}, Na^{+}, HCO_3^-, NO_3^-, and Cl^- show no statistically significant variations.

The average concentrations of heavy metals follow the order: Fe (2.2 mg/l) > Cu (1 mg/l) > Zn (0.4 mg/l) > Mn (0.3 mg/l) (Table S5). Fe and Mn concentrations exceed WHO standards (0.3 mg/l and 0.1 mg/l, respectively), posing risks to human health and ecosystems (Fig. 8).

3.4. Water typology and hydrogeochemical processes

The typology of water samples was analyzed using Piper and Chadha diagrams (Fig. 9). The different water facies identified are summarized in Table S6. According to the Piper diagram (Fig. 9a), Lake Guiers' waters are predominantly dominated by mixed-HCO_3, Ca-HCO_3, and Na-HCO_3 water types. The Chadha plot (Fig. 9b) classifies most samples as fresh (mixed-HCO_3 type, Field 5), as already depicted with the Piper diagram. Only a few samples collected during March and February (dry season) and October (rainy season) exhibit Ca-Mg-SO_4/Cl type (Field 6) and Na-Cl type (Field 7), indicating anthropogenic salinity.

The Fields 6 and 7 correspond to waters affected by agricultural drainage and industrial effluents (Fig. 9c). Samples in Field 8 (Na-HCO_3), observed during the rainy season, may reflect rainwater inputs naturally enriched with Na^{+} and HCO_3^- through atmospheric CO_2 dissolution. Additionally, watershed lithology and soil classes can contribute to ionic enrichment.

3.5. Multivariate statistical analysis

3.5.1. Correlation and principal component analysis

Both the correlation matrix analysis and Principal Component Analysis (PCA) were applied to the sixteen physicochemical parameters measured over the different sampling campaign months (Figs. 10 and 11). The correlation matrix analysis reveals strong positive correlations between Ca^{2+}, Mg^{2+}, Na^{+}, K^{+}, HCO_3^-, Cl^-, and SO_4^{2-} ions and electrical conductivity (EC) ($r = 0.75$–0.95) across all months, except for February. These correlations confirm that dissolved salts significantly contribute to water mineralization.

Suspended matter shows a strong positive correlation with Ca^{2+}, Mg^{2+}, Na^{+}, K^{+} ions ($r = 0.66$–0.80) in May and with SO_4^{2-}, HCO_3^-, and Ca^{2+} ($r = 0.80$) in March. Cyanobacteria concentrations exhibit a strong positive correlation with SPM ($r = 0.97$) in May and a significant negative correlation ($r = -0.64$) in February. Dissolved oxygen (DO) shows a significant positive correlation with temperature ($r = 0.71$) in May and a negative correlation ($r = -0.71$) in March, as well as with turbidity ($r = -0.61$) in August. Temperature was positively correlated with chlorophyll-a ($r = 0.70$) in May and with pH ($r = 0.74$) in February.

In parallel, PCA reduced data complexity by extracting key components. The first two principal dimensions were selected on the

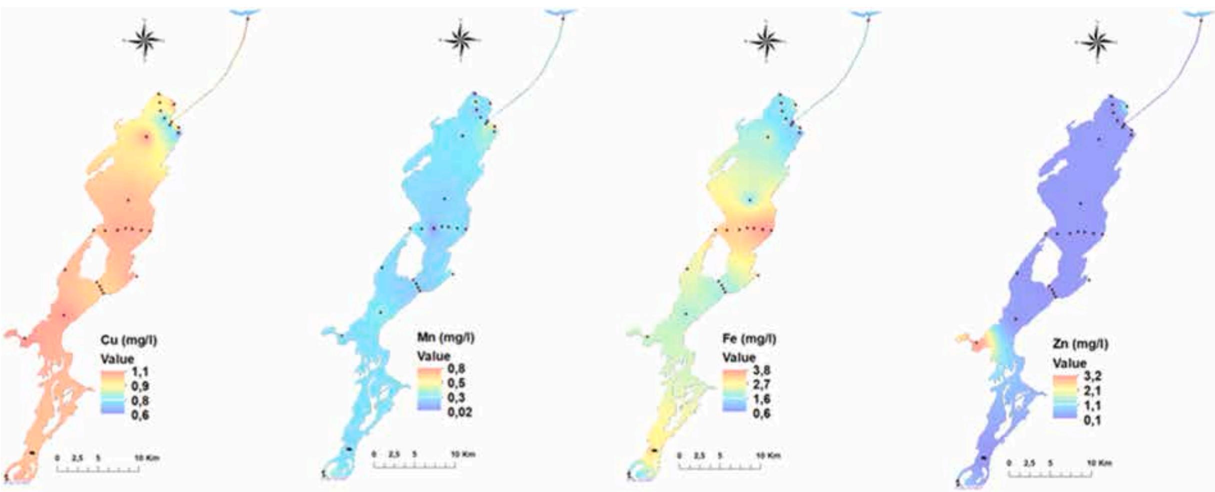

Fig. 8. Spatial distribution of four heavy metals detected in February 2023 in Lake Guiers.

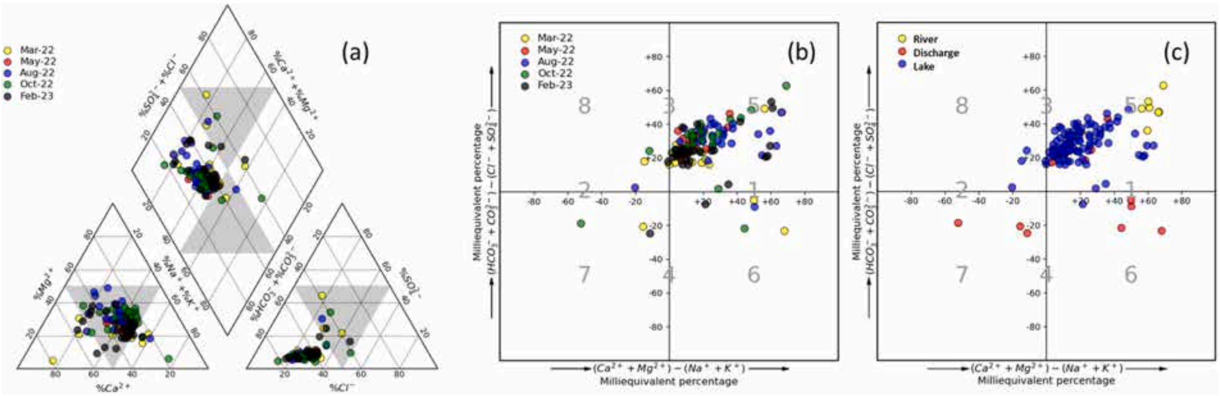

Fig. 9. Water facies composition by month: (a) Piper diagram and (b) Chadha plot by month and (c) by source defining Fields (1) Alkaline earths exceed alkali metals, (2) Alkali metals earths exceed alkaline earths, (3) Weak acid anions exceed strong acid anions, (4) Strong acid anions exceed weak acid anions, (5) Ca-Mg-HCO3-type refills, (6) Ca-Mg-SO4/Cl, (7) Na-Cl and (8) Na-HCO3-type basic ion-exchange waters.

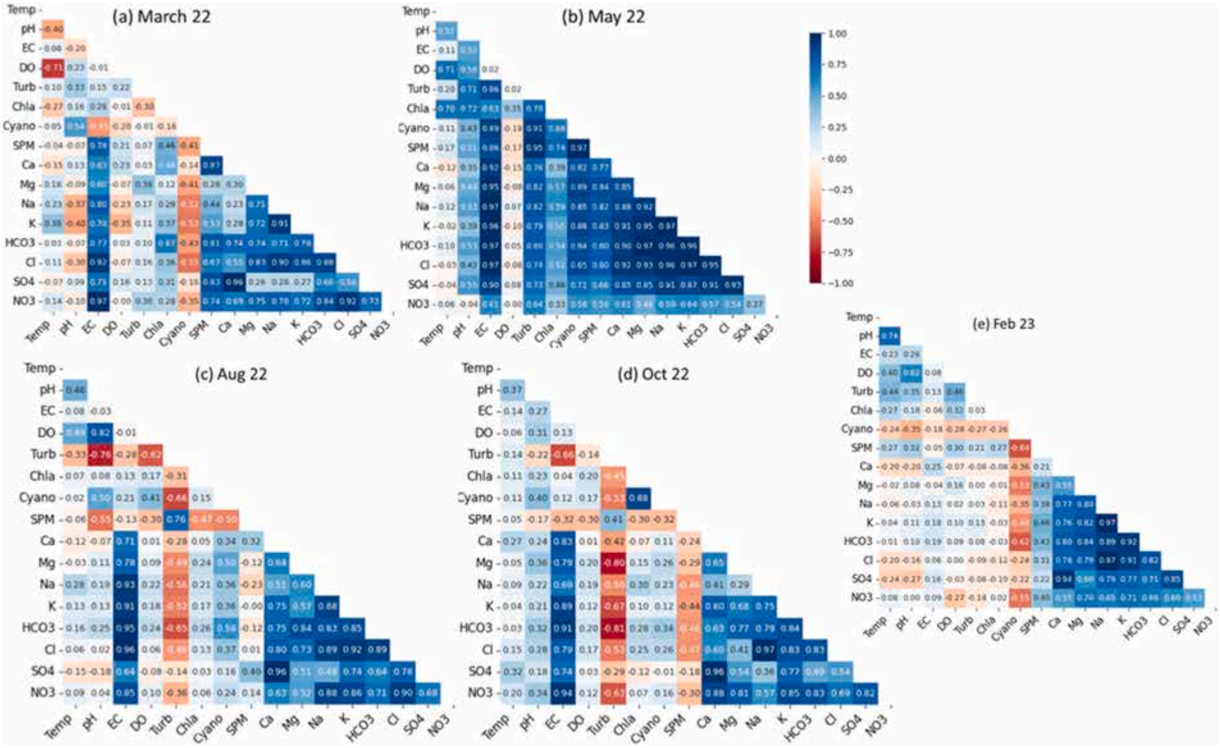

Fig. 10. Correlation coefficients between water parameters in (a) March, (b) May, (c) August, (d) October and (e) February.

basis of eigenvalue criteria (eigenvalues ≥ 1), covering 67.5 %, 83.1 %, 72.2 %, 64.6 %, and 63.8 % of the total variance in March, May, August, October, and February, respectively (Fig. 8). The loading values (cos^2) were classified as "strong" (> 0.75), "moderate" (0.75–0.50), and "weak" (0.50–0.30), respectively.

The first principal component (PCA1) was dominated during the dry season (March, May, February) by positive loadings for Na^+, Cl^-, Mg^{2+}, K^+, HCO_3^-, EC, and SO_4^{2-}. This observation aligns with the strong positive correlations observed in the correlation matrix. The onset of rains in August maintained a similar influence (PCA1), now accompanied by strong correlations with NO_3^- and turbidity. At the end of the wet season in October, when water levels peak, a new dimension emerges with PCA2, characterized chl-a and cyanobacteria. In contrast, PCA1 shows strong negative loadings with turbidity and moderate positive loadings with HCO_3^-, NO_3^-, and SO_4^{2-}. In February, marking the return to the dry season, PCA1 remains dominated by major ions and electrical conductivity.

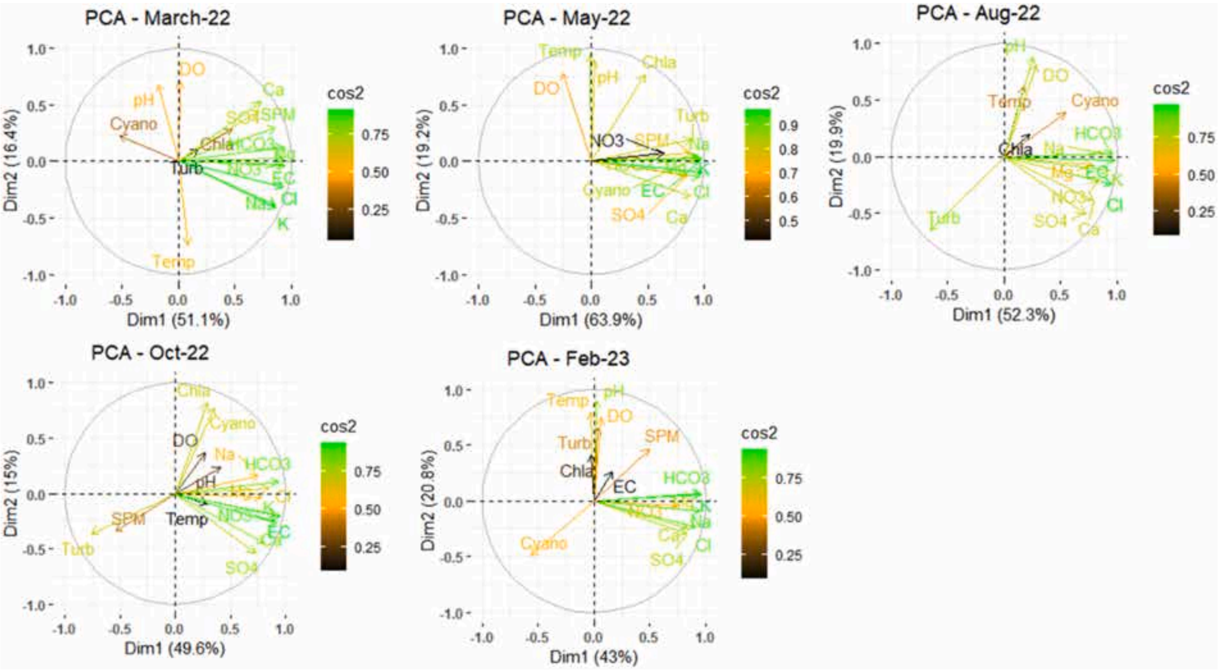

Fig. 11. Principal component analysis of ions in lake water.

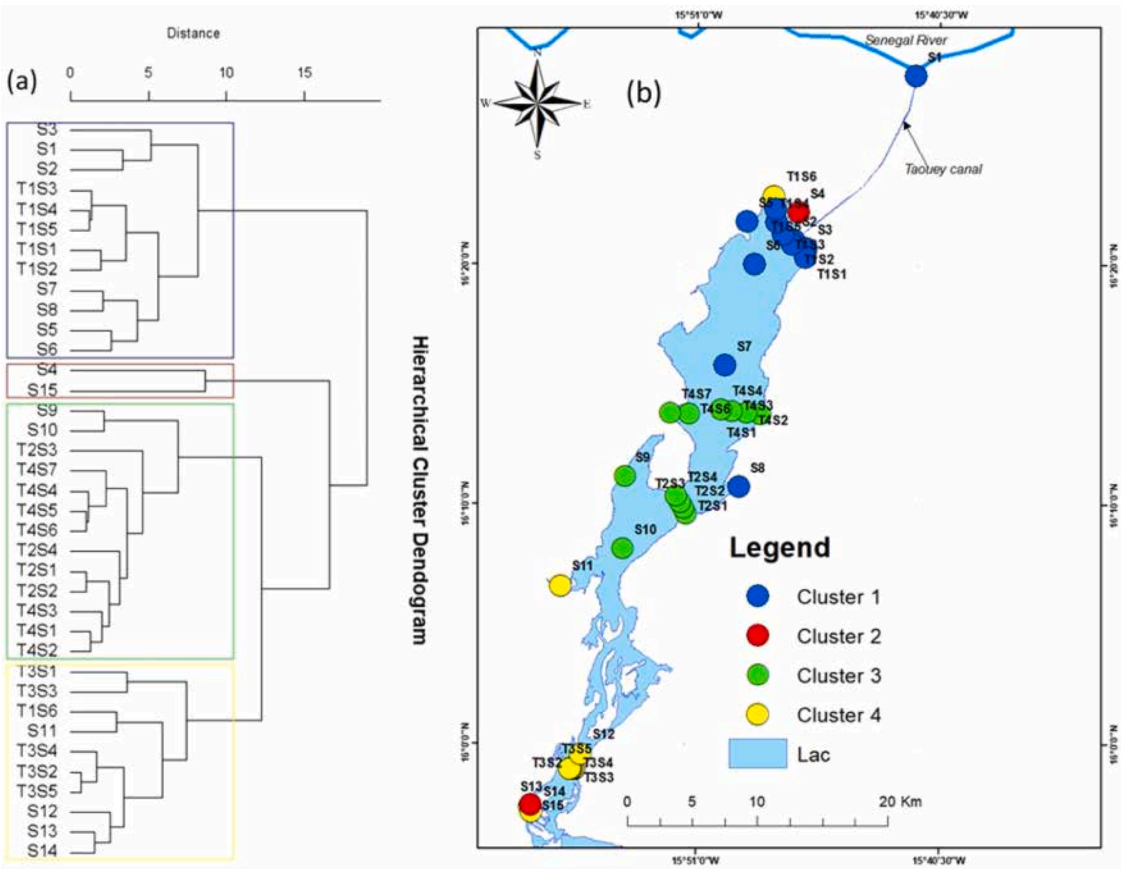

Fig. 12. HCA results: a) identification of the groups in the dendrogram and b) spatial distribution of the clusters.

3.5.2. Hierarchical cluster analysis

The Hierarchical Clustering Analysis (HCA) is represented as a dendrogram (e.g., Vasistha and Ganguly, 2024). HCA was used to group sampling sites with similar water quality characteristics. Seasonal median values of the measured parameters were utilized. The results reveal an organization of the sites into four distinct clusters (Fig. 12).

Most sites in Cluster 1, located in the northern part of the lake near the Taouey Canal, exhibit high turbidity (86.2 NTU). Cluster 2 primarily includes sites near agricultural discharges (northern zone) and industrial effluents (southern zone), showing the highest conductivity values and maximum concentrations of TOC and Chl-a. Cluster 3 sites, situated in the central zone, combine intermediate concentrations (SPM, HCO_3^-) and moderate algal proliferation. Finally, Cluster 4 sites, located in the southern part of the lake, are distinguished by heightened mineralization. These four clusters reflect distinct hydrological, anthropogenic, and biochemical processes which are discussed in Section 4 in light of the results from the samples and the statistical analyses.

3.6. Drinking water quality assessment and irrigation suitability

The Water Quality Index (WQI) computation based on 13 water quality parameters measured over five periods is presented in Table 3. The analysis reveals a concerning decline in water quality over the rainy season. Values averaged 127.8 (March), 125.1 (May), 374.4 (August), 205.3 (October), and 121.2 (February), categorizing most samples as poor to unsuitable for human consumption.

Seasonal variability is stark: August 2022 marked the worst conditions, with 39.5 % of samples deemed "unsuitable for drinking," likely due to flood-induced sediment and pollutant influx from the Senegal River basin. Conversely, October 2022 showed slight improvement (21.1 % very poor), possibly reflecting post-flood dilution. However, the majority of samples consistently fell into the poor category (66.7–86.7 %).

The quantity and variety of crops cultivated, soil health, and environmental sustainability all depend heavily on irrigation water quality. Therefore, evaluating this quality is essential, particularly through indicators such as Sodium Percentage (%Na). The calculated SSP values for irrigation suitability range from 15.43 % to 76.13 %, with an average of 39.86 % over five seasons. The highest values were recorded in an area receiving discharges upstream of the lake, raising concerns. According to Wilcox diagram (Fig. 13), all water samples across different seasons fall within the excellent to good categories, indicating that most samples are suitable for agricultural irrigation.

4. Discussion

Extensive monitoring throughout Lake Guiers during five campaigns conducted between March 2022 and February 2023 revealed marked spatio-temporal variability in water quality, confirming and expanding upon previous findings on the lake (Diédhiou et al., 2019; Sane et al., 2015; Cogels et al., 1993). The approach used in this study, combining classical and multivariate statistical analyses, enabled a better understanding of the combined effects of human activities and natural factors on water quality a critical need still largely unmet in many regions worldwide. Hierarchical cluster analysis (HCA) (Fig. 12), applied to detect spatial similarity between monitoring sites (Egbueri and Mgbenu, 2020), identified four spatial groups, each marked by specific hydrochemical conditions and varying degrees of anthropogenic influence. Cluster 1 includes sites located in the northern part of the lake and one site situated centrally, on the left bank, within an irrigation canal. The northern sites receive turbid and weakly mineralized river water (Fig. 6), due to their proximity to the Taouey Canal, which carries large sediment loads during floods (Sane et al., 2015). Peaks in turbidity and suspended solids are particularly high in August. These sediment inputs originate mainly from the Senegal River and are enhanced by occasional soil leaching in the watershed. Runoff from the surrounding watershed is estimated to be moderate, except for extreme rainfall events as observed on August 25 2022 (101 mm). During the lake's filling phase when river flows are high, fine particles (clay, silt) are temporarily suspended by turbulent currents, especially in northern and central zones, before gradually settling as flows decrease toward the south. Rapid sedimentation, driven by reduced flow velocity (< 0.034 m/s) (Sane et al., 2015), explains the progressive decline in turbidity downstream. As for the site in the irrigation canal on the left bank, its specificity lies in its position within a drainage system, making it strongly influenced by agricultural runoff from upstream.

Cluster 2 includes sites located in the northern and southern parts of the lake, influenced respectively by agricultural discharges and industrial effluents. These sites are characterized by high levels of CE, Na^+, Cl^-, SO_4^{2-}, and TOC, as well as high concentrations of Chl-a, indicating nutrient enrichment and increased biological productivity (Fig. 6). Some sites (e.g., S5, S8, T3S1) also show high pH values (>8.5), reflecting both natural processes (photosynthesis, organic matter decomposition) and anthropogenic pressures (agricultural and domestic effluents). The hydrochemical facies identified in these zones (Fig. 9c) correspond to Ca-Mg-SO_4/Cl and Na-Cl types,

Table 3
Water Quality Index (WQI) results for five months (March 2022 - February 2023) and % are the number and percentage of sample, respectively.

		March-22		May-22		Aug −22		Oct- 22		Feb −23	
Water classification	**WQI Values**	**n**	**%**	**n**	**%**	**n**	**%**	**n**	**%**	**n**	**%**
Excellent water	< 50	0	0.00	0	0.00	0	0.00	0	0.00	0	0
Good water	50–100	2	13.33	5	33.33	3	7.89	11	28.95	9	26.47
Poor water	100.1–200	13	86.67	10	66.67	17	44.74	10	26.32	25	73.53
Very poor water	200.1–300	0	0.00	0	0.00	3	7.89	8	21.05	1	2.94
Unsuitable for drinking purposes	> 300	0	0.00	0	0.00	15	39.47	9	23.68	0	0

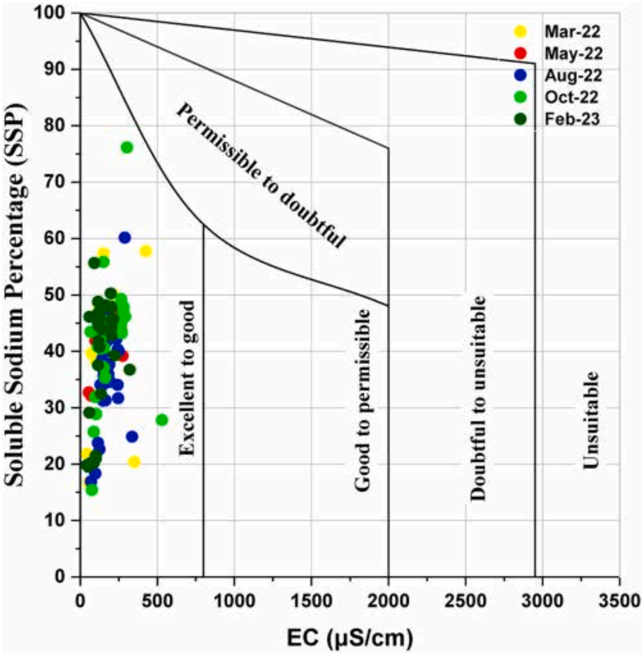

Fig. 13. Suitability of lake water for irrigation according to the Wilcox diagram.

which indicate anthropogenic salinization (Kazi et al., 2009). This chemical composition aligns with the inputs of sulfates and chlorides from fertilizers and industrial discharges. The historical use of gypsum ($CaSO_4 \cdot 2H_2O$) by the local sugar company for soil desalination in irrigated areas may also explain the elevated SO_4^{2-} and Cl^- concentrations observed in this zone (Cogels et al., 1993). Furthermore, these sites also show contamination by metallic ions such as Fe and Mn, reflecting anthropogenic activities (wastewater discharges and agricultural fertilizers) (Chen et al., 2016; Xiao et al., 2020). These metals were measured at four sites in the lake in February 2017 (Niang et al., 2017), with average concentrations of 0.0913 mg/l for Fe and 0.0013 mg/l for Mn. In comparison, measurements from the same sites in February 2023 reveal a significant increase in average concentrations, reaching 1.88 mg/l and 0.45 mg/l for Fe and Mn, respectively. This increase during the dry season is attributed to a combination of metal release from bottom sediments due to redox processes and localized wastewater discharges. Similar observations have been made on Lake Tana in Ethiopia (Sishu et al., 2024). Moreover, solid waste dumping and burning near the lake can exacerbate pollution levels. A similar situation was documented in the Çavuşlu stream in Turkey, where proximity to a waste disposal facility led to significant degradation of water quality, especially with elevated Fe and Mn concentrations linked to anthropogenic pressures (Yuksel et al., 2021). This highlights the urgent need for regular monitoring of both surface water and drinking water quality to avoid chronic toxic exposure among local populations. In addition, the iron-rich tropical ferruginous soils bordering the lake can release iron into the lake waters, especially in the event of runoff or erosion.

Cluster 3 includes sites located in the central part of the lake, with intermediate concentrations of suspended solids and bicarbonates, as well as moderate algal proliferation. These conditions suggest limited water circulation and mixed inputs (natural and anthropogenic). This situation may seem reassuring for the drinking water intake area at Ngnith, located in this zone. However, this apparent stability remains fragile in light of upstream changes. This highlights the importance of reinforced monitoring to anticipate potential impacts on the quality of water for human consumption.

Cluster 4 is located in the southern part of the lake and is marked by high mineralization, especially during the dry season. This is explained by a combination of hydrological and geochemical processes: high evaporation rates (~5.5 mm/day) and water level decline (2.18 m) promote progressive ion concentration. This situation is also partly linked to stagnant water volumes in this zone, which may limit water renewal. Additionally, aquatic vegetation in this zone slows currents and traps sediments, enhancing mineral precipitation and retention. PCA (Fig. 11) confirms this trend with persistent saline loads during the dry season. This thermal and chemical configuration is typical of Sahelian lakes, where surface waters respond quickly to atmospheric conditions, particularly during the rainy season marked by increased humidity and cloud cover affecting heat exchange (Khadija et al., 2021). The observed mineral signature—especially chemical facies rich in Ca^{2+}, Mg^{2+}, SO_4^{2-}, and Cl^-—could result from the dissolution of local geological formations such as limestone, marl, and gypsum. Similar processes have been observed in the Jajrood River in Iran (Razmkhah et al., 2010). The geological context of Lake Guiers, characterized by Quaternary marine deposits (limestone, marl) and ferruginous formations (Niang et al., 2022), supports this hypothesis. Additionally, the presence of mixed facies indicates active ion exchange and contributions from both diffuse sources (agricultural runoff, soil leaching) and point sources (drainage, effluents). Such mechanisms have been described in other semi-arid basins, notably by Saleem et al. (2015).

The spatiotemporal diversity observed across the different clusters illustrates the complexity of the hydrogeochemical functioning of Lake Guiers. This heterogeneity is particularly marked by gradients in mineralization, turbidity, nutrients, and organic matter, depending on location and hydrological season. This classification, based on hydrological mechanisms and hydrochemical regulatory factors, highlights the high vulnerability of this lacustrine system. This dynamic is clearly reflected in the principal component analysis (PCA) (Fig. 11), which highlights two dominant chemical regimes. During the dry season, the high mineralization (PCA1), already identified in Cluster 4, is confirmed by the association of elements such as sodium, chlorides, and sulfates. This composition indicates a mixed natural and anthropogenic origin—a phenomenon also observed in the arid Beichuan River Basin in northwestern China (Xiao et al., 2020) and the semi-arid High Ziz area in southeastern Morocco (Khadija et al., 2021). During the rainy season (August–October), the PCA revealed two important findings. In August, the PC2 axis reflects an active biological process, marked by a strong positive correlation between temperature, pH, and dissolved oxygen, corresponding to intense photosynthesis during the algal bloom period. Turbidity, negatively correlated with PC2 in both periods, suggests that areas where these biological processes are most active also have lower concentrations of suspended particles.

This observation aligns with the conditions previously described in clusters 3 and 4, characterized by low turbidity associated with increased mineralization. Moreover, the hypothesis that the central and southern parts of the lake are eutrophic was suggested by Diédhiou et al. (2019), who observed low chlorophyll-a concentrations during cold and wet seasons ($\leq$13–14 μg/l in January and September) and peaks during warm periods ($\geq$14–15 μg/l in May), thus classifying the lake as "oligo-mesotrophic" in the wet season and "eutrophic" in the dry season— a trend similar to our findings. Surface water warming creates favorable conditions for algal proliferation, as demonstrated by Wu et al. (2022) in their study of 21 lakes, where water temperature was found to be a major regulating factor of chlorophyll-a. The accumulation and subsequent runoff of nutrients into the lake, driven by seasonal surface runoff and soil leaching, further stimulates algal growth, as documented by Kazi et al. (2009) and Kale et al. (2021) in other agriculture-influenced watersheds. This phenomenon reflects a major negative effect of eutrophication, generating environmental and health risks (Søndergaard et al., 2011). It is therefore clear that the lake's algal dynamics are partly linked to its seasonal hydroclimatic regime and highlight the need for enhanced monitoring, notably through satellite imagery, to better track its evolution.

Regarding implications for public health and irrigation, the results calculated over five sampling campaigns indicate a water quality that is generally acceptable for irrigation, but that raises concerns for drinking water supply. The Water Quality Index (WQI) (Table 3) revealed alarming seasonal degradation, particularly in August, when nearly 40 % of the samples were deemed unfit for human consumption. These findings are consistent with trends observed in other African lakes impacted by agricultural and urban runoff, such as Lake Magadi in Kenya (WQI = 158.8), Lake Elementaita (WQI = 128.4), Lake Bogoria (WQI = 79.5) (Githaiga et al., 2021), and Lake Tana in Ethiopia ($75 \leq$ WQI < 100) (Sishu et al., 2024). These results underscore the urgent need to implement proactive management strategies to minimize both diffuse and point-source inputs into Lake Guiers. Such actions would in turn help reduce the high prevalence of waterborne diseases (diarrhea, helminthiasis), urinary tract infections, dysentery, hematuria, schistosomiasis, and bloody stools, to which the local population is regularly exposed (Diop, 2013). From an agricultural standpoint, the sodium percentage (Na%) values presented in the Wilcox diagram (Fig. 13) ranged from 15.43 % to 76.13 %, with an average of 39.86 %, all below the 80 % threshold (classified as unsuitable for irrigation). These results therefore indicate that the lake water is generally acceptable for irrigation. They are consistent with those observed in other regions, such as the Giresun Province in Türkiye, where spring waters were found to be suitable for irrigation based on multiple indicators, including Na%, Sodium Adsorption Ratio (SAR), Total Dissolved Solids (TDS), and Electrical Conductivity (EC), with mean values below recommended thresholds (Karadeniz et al., 2024). Similarly, in the Gökpınar Basin (Taşdelen, 2021), spring waters showed favorable irrigation parameters, including a Na % well below the critical limits (<80 %). Comparable results were also reported in humid tropical environments, such as the Ethiopia River Basin in Nigeria, where Na% values remained within acceptable irrigation classes ($20 <$ Na% ≤ 80) according to established standards (Ushurhe et al., 2024).

This study highlights the need to assess the combined effects of human activities and natural factors on water quality. Although five campaigns were conducted, which is sufficient to capture major seasonal fluctuations, some limitations remain. Long-term data is important to identify the impact of extreme variations in rainfall and lake inflow over time, while continuous monitoring may help capture ephemeral pollution events at some of the locations identified here. Further sampling which coincides with cloud-free satellite imagery could also help identify the potential of remote monitoring for parameters including turbidity and chlorophyll-a (Bid and Siddique, 2019; Danaher et al., 2022). In addition, with additional funding, additional toxic metals and microbiological or bacteriological parameters could be included, as well as targeted pesticide analysis.

5. Conclusion

This study provides a comprehensive evaluation of Lake Guiers' water quality through an integrated approach combining multivariate statistics, hydrogeochemical methods and hydroclimatic monitoring. The results demonstrate that several parameters exceed the thresholds recommended by the USEPA and WHO, particularly for cyanobacteria, chlorophyll-a, turbidity, organic matter, iron, and manganese concentrations. These exceedances present significant challenges for water treatment processes necessary to ensure safe drinking water. Currently, there are no specific national standards for these parameters. Establishing locally adapted guidelines would be a relevant step toward improving water quality monitoring and management in such a critical resource.

The hydrochemistry of the lake is generally characterized by a progressive north-to-south mineralization gradient that persists regardless of season. Temporal variations are primarily influenced by evaporation during the dry season, agricultural drainage, and the combination of runoff and inflow waters during the rainy season. Furthermore, the investigation revealed that chlorophyll-a levels peak during the hot season, driven by favorable higher temperatures, and hydrodynamic mixing, while cyanobacteria proliferation occurs predominantly during the rainy season in response to the increased availability of bioavailable nutrients. However, greater concentrations of turbidity and suspended particulate matter were observed in the north of the lake, as a result of sediment-loaded inflow from the Taouey canal. Finally, the Water Quality Index (WQI) analysis indicates that the current quality of Lake Guiers' water ranges from poor to unsuitable for consumption across many sampling locations and periods.

These findings underscore the urgent need for targeted interventions to reduce pollution sources and implement sustainable management practices, considering the strategic important of Lake Guiers for national drinking water supply and agricultural production. The lake is increasingly solicited to meet Senegal's long-term development objectives through several major projects. These include the PREFERLO project—which aims to mobilize Lake Guiers' water for irrigation, domestic supply, and livestock watering to enhance ecosystem resilience in the Lower Ferlo (OLAC, 2021)—and the Grand Water Transfer Project (GTE), designed to further supply the capital and other previously underserved areas by 2035, with strategic planning extending toward 2050 (World Bank, 2022).

Furthermore, the research highlights the interplay between natural factors and anthropogenic influences, particularly the impacts of intensified agriculture and wastewater discharge on water quality. Domestic waste discharge points and agricultural drainage outlets located near the lake should be relocated to minimize contamination risks. The limited contribution of local runoff events compared to river inflows underlines the importance of the Taouey canal in determining lake levels, and accordingly seasonal changes in water quality. Accordingly future research must help identify the impact of changes in lake water inflow on pollutant dilution and transport processes. Similarly, continuous monitoring of pollution levels by local authorities at selected locations must help identify the contribution of ephemeral local runoff and transitory drainage to localized pollution events. Integrated approaches involving multiple stakeholders and awareness campaigns targeting local populations are required to define long term management strategies and preserve the fragile equilibrium of freshwater lakes in semi-arid areas.

CRediT authorship contribution statement

Abib Ndiaye: Methodology, Data curation. **Johann Bellanger:** Supervision, Funding acquisition. **Oumy Tall:** Methodology, Data curation. **Didier Martin:** Methodology, Data curation. **Andrew Ogilvie:** Writing – review & editing, Supervision, Funding acquisition. **Djim M.L Diongue:** Writing – review & editing, Visualization, Formal analysis, Conceptualization. **Hikimat Saadi:** Writing – original draft, Methodology, Formal analysis, Conceptualization. **Serigne Faye:** Writing – review & editing, Supervision, Funding acquisition.

Declaration of Competing Interest

The authors declare that they have no known competing financial interests or personal relationships that could have appeared to influence the work reported in this paper.

Acknowledgements

The authors would like to express their sincere gratitude to the Senegalese Water Company (SEN'EAU), the French National Research Institute for Sustainable Development (IRD), Lake Guiers and Watercourses Office (OLAC) and the Doctoral School for Water, Water Quality, and Usage (EDEQUE) at Cheikh Anta Diop University in Dakar (UCAD) for their technical and financial support to this PhD research program. We also wish to thank the Editors and Reviewers for their valuable comments and suggestions which improved the quality of this manuscript

Appendix A. Supporting information

Supplementary data associated with this article can be found in the online version at doi:10.1016/j.ejrh.2025.102695.

Data availability

Data will be made available on request.

References

Ayele, H.S., Atlabachew, M., 2021. Review of characterization, factors, impacts, and solutions of lake eutrophication: lesson for lake tana, Ethiopia. Environ. Sci. Pollut. Res. 28 (12), 14233–14252. https://doi.org/10.1007/s11356-020-12081-4.

Bader, J.C., 2015. Monographie hydrologique du fleuve Sénégal: de l'origine des mesures jusqu'en 2011. IRD editions, Montpellier, France.

Bah, A., Diallo, R., Faye, S., & Vanclooster, M. (2022). Pesticide residues accumulation in freshwater, sediments, and fish in the Guiers Lake basin: Risks for Senegal's strategic water reservoir. *South African Hydrological Society*.

Bangani, L., Kabiti, H.M., Amoo, O., Nakin, M.D.V., Magayiyana, Z., 2023. Impacts of illegal solid waste dumping on the water quality of the mthatha river. Water Pract. Technol. 18 (5), 1011–1021. https://doi.org/10.2166/wpt.2023.053.

Benam-Beltoungou, E.Y.T., Bassene, I., Emvoutou, H.C., Akpataku, K.V., Diongue, D.M.L., Faye, S., 2025. Groundwater quality assessed using water quality indices and geostatistical methods in the thiaroye aquifer, Senegal. water. Science 39 (1), 151–170.

Bhat, R.A., Singh, D.V., Qadri, H., Dar, G.H., Dervash, M.A., Bhat, S.A., Unal, B.T., Ozturk, M., Hakeem, K.R., Yousaf, B., 2022. Vulnerability of municipal solid waste: an emerging threat to aquatic ecosystems. Chemosphere 287, 132223. https://doi.org/10.1016/j.chemosphere.2021.132223.

Bid, S., Siddique, G., 2019. Identification of seasonal variation of water turbidity using NDTI method in panchet hill dam, India. Model. Earth Syst. Environ. 5 (4), 1179–1200. https://doi.org/10.1007/s40808-019-00609-8.

Bruckmann, L., Ogilvie, A., Martin, D., Diakhaté, F.B., Tilmant, A., 2025. Mapping seasonal flood-recession cropland extent in the Senegal river valley. Remote Sens. Appl. Soc. Environ., 101473

Chadha, D.K., 1999. A proposed new diagram for geochemical classification of natural waters and interpretation of chemical data. Hydrogeol. J. 7 (5), 431–439. https://doi.org/10.1007/s100400050216.

Chen, M., Qin, X., Zeng, G., Li, J., 2016. Impacts of human activity modes and climate on heavy metal "spread" in groundwater are biased. Chemosphere 152, 439–445. https://doi.org/10.1016/j.chemosphere.2016.03.046.

Chidiac, S., El Najjar, P., Ouaini, N., El Rayess, Y., El Azzi, D., 2023. A comprehensive review of water quality indices (WQIs): history, models, attempts and perspectives. Rev. Environ. Sci. Bio/Technol. 22 (2), 349–395. https://doi.org/10.1007/s11157-023-09650-7.

Cogels F.X., Gac J.Y. (1981) - Le lac de Guiers: Fonctionnement, bilans hydriques, évaporation d′une nappe d′eau libre en zone sahélienne (Sénégal). Cah. ORSTOM, série Géologie, vol. VII, n° 1, pp. 41-60.

Cogels, F.X., Niang, A., Carn, M., and Gac J.Y. (1993). Recherche d'une station de référence pour un suivi qualitatif régulier des eaux du lac de Guiers, Rapport Orstom-Dakar, EEC (EQUESEN programme). 15 pp.

Cogels, F.X., Coly, A., Niang, A., 1997. Impact of dam construction on the hydrological regime and quality of a sahelian lake in the river Senegal basin. Regul. River. Res. Manag. 13 (1), 27–41. https://doi.org/10.1002/(SICI)1099-1646(199701)13:1<27::AID-RRR421>3.0.CO;2-G.

Cogels, F.-X., Fraboulet-Jussila, S., Varis, O., 2001. Multipurpose use and water quality challenges in lac de guiers (Senegal). Water Sci. Technol. 44 (6), 35–46. https://doi.org/10.2166/wst.2001.0335.

Crossman, J., Futter, M.N., Elliott, J.A., Whitehead, P.G., Jin, L., Dillon, P.J., 2019. Optimizing land management strategies for maximum improvements in lake dissolved oxygen concentrations. Sci. Total Environ. 652, 382–397. https://doi.org/10.1016/j.scitotenv.2018.10.160.

Danaher, C., Newbold, T., Cardille, J., Chapman, A.S.A., 2022. Prioritizing conservation in sub-Saharan African lakes based on freshwater biodiversity and algal bloom metrics. Conserv. Biol. 36 (5), e13914. https://doi.org/10.1111/cobi.13914.

Diédhiou, C., Diop, S., Faye, G., Moshod, T., Wade, S., 2019. Study on the applicability of Landsat-8 images as a tool for monitoring the trophic state of lake guiers (Senegal). J. Water Resour. Prot. 11 (04), 434–447. https://doi.org/10.4236/jwarp.2019.114026.

Diongue, D.M., Sagnane, L., Emvoutou, H., Faye, M., Gueye, I.D., Faye, S., 2022. Evaluation of groundwater quality in the deep maastrichtian aquifer of Senegal using multivariate statistics and water quality index-based GIS. J. Environ. Prot. 13 (11), 819–841.

Diop, A., 2013. *diagnostic des pratiques d'utilisation et quantification des pesticides dans la zone des niayes de dakar (sénégal)*. Université du littoral Côte d'Opale. Français. MNNT 2013, 2013DUNK0341. tel-00959895.

Downing, J.A., Watson, S.B., McCauley, E., 2001. Predicting Cyanobacteria dominance in lakes. Can. J. Fish. Aquat. Sci. 58 (10), 1905–1908. https://doi.org/10.1139/f01-143.

Egbueri, J.C., Mgbenu, C.N., 2020. Chemometric analysis for pollution source identification and human health risk assessment of water resources in ojoto province, southeast Nigeria. Appl. Water Sci. 10 (4). https://doi.org/10.1007/s13201-020-01180-9.

Ekholm, P., Mitikka, S., 2006. Agricultural lakes in Finland: current water quality and trends. Environ. Monit. Assess. 116 (1-3), 111–135. https://doi.org/10.1007/s10661-006-7231-3.

Englert, D., Zubrod, J.P., Schulz, R., Bundschuh, M., 2015. Variability in ecosystem structure and functioning in a low order stream: implications of land use and season. Sci. Total Environ. 538, 341–349. https://doi.org/10.1016/j.scitotenv.2015.08.058.

Fantong, W.Y., Kamtchueng, B.T., Yamaguchi, K., Ueda, A., Issa, Ntchantcho, R., Wirmvem, M.J., Kusakabe, M., Ohba, T., Zhang, J., Aka, F.T., Tanyileke, G., Hell, J. V., 2015. Characteristics of chemical weathering and water–rock interaction in lake nyos dam (Cameroon): implications for vulnerability to failure and re-enforcement. J. Afr. Earth Sci. 101, 42–55. https://doi.org/10.1016/j.jafrearsci.2014.08.011.

Gaury, P.K., Meena, N.K., Mahajan, A.K., 2018. Hydrochemistry and water quality of rewalsar lake of lesser himalaya, himachal pradesh, India. Environ. Monit. Assess. 190 (2), 84. https://doi.org/10.1007/s10661-017-6451-z.

Githaiga, K.B., Njuguna, S.M., Gituru, R.W., Yan, X., 2021. Water quality assessment, multivariate analysis and human health risks of heavy metals in eight major lakes in Kenya. J. Environ. Manag. 297, 113410. https://doi.org/10.1016/j.jenvman.2021.113410.

González, P.S., Stehr, A., Barra, R.O., 2024. Assessment of water quality trends through the application of an aggregated water quality index with historical monitored data in a Mediterranean andean basin. Ecol. Indic. 166, 112373. https://doi.org/10.1016/j.ecolind.2024.112373.

Guenouche, F.Z., Mesbahi-Salhi, A., Zegait, R., Chouia, S., Kimour, M.T., Bouslama, Z., 2024. Assessing water quality in North-East Algeria: a comprehensive study using water quality index (WQI) and PCA. Water Pract. Technol. 19 (4), 1232–1248. https://doi.org/10.2166/wpt.2024.073.

Holopainen, S., Lehikoinen, A., 2022. Role of forest ditching and agriculture on water quality: connecting the long-term physico-chemical subsurface state of lakes with landscape and habitat structure information. Sci. Total Environ. 806, 151477. https://doi.org/10.1016/j.scitotenv.2021.151477.

Institut Sénégalais de Normalisation (ISN). (2001). NS 05-061 - Eaux usées: Normes de rejet. Dakar, Sénégal: ISN. (Source: Direction de l'Environnement et des Établissements Classés).

Jiang, Y., He, K., Li, Y., Qin, M., Cui, Z., Zhang, Y., Yao, Y., Chen, X., Deng, M., Gray, A., Li, B., 2022. Driving factors of total organic carbon in danjiangkou reservoir using generalized additive model. Article 6. Water 14 (6). https://doi.org/10.3390/w14060891.

Kâ, S., Pagano, M., Bâ, N., Bouvy, M., Leboulanger, C., Arfi, R., Thiaw, O.T., Ndour, E.H.M., Corbin, D., Defaye, D., Cuoc, C., Kouassi, E., 2006. Zooplankton distribution related to environmental factors and phytoplankton in a shallow tropical lake (Lake Guiers, Senegal, West Africa). Int. Rev. Hydrobiol. 91 (5), 389–405. https://doi.org/10.1002/iroh.200610863.

Kaiser, H.F., 1960. The application of electronic computers to factor analysis. Educ. Psychol. Meas. 20, 141–151.

Kale, A., Bandela, N., Kulkarni, J., Sahoo, S.K., Kumar, A., 2021. Hydrogeochemistry and multivariate statistical analysis of groundwater quality of hard rock aquifers from deccan trap basalt in Western India. Environ. Earth Sci. 80 (7), 288. https://doi.org/10.1007/s12665-021-09586-7.

Kalny, G., Laaha, G., Melcher, A., Trimmel, H., Weihs, P., Rauch, H.P., 2017. The influence of riparian vegetation shading on water temperature during low flow conditions in a medium sized river. Article 418. Knowl. Manag. Aquat. Ecosyst. 418. https://doi.org/10.1051/kmae/2016037.

Kamara, S., Martin, P., Coly, A., 2021. Transfert d'eau et développement urbain dans le bassin aval du fleuve Sénégal. Open Access 3.

Karadeniz, S., Ustaoğlu, F., Aydın, H., et al., 2024. Toxicological risk assessment using spring water quality indices in plateaus of giresun Province/Türkiye: a holistic hydrogeochemical data analysis. Environ. Geochem Health 46, 285. https://doi.org/10.1007/s10653-024-02054-8.

Kazi, T.G., Arain, M.B., Jamali, M.K., Jalbani, N., Afridi, H.I., Sarfraz, R.A., Baig, J.A., Shah, A.Q., 2009. Assessment of water quality of polluted lake using multivariate statistical techniques: a case study. Ecotoxicol. Environ. Saf. 72 (2), 301–309. https://doi.org/10.1016/j.ecoenv.2008.02.024.

Khadija, Diani, Hicham, Amar, Rida, Azmi, Hicham, Elbelrhiti, Nordine, Nouayti, Najlaa, Fathi, 2021. Surface water quality assessment in the semi-arid area by a combination of heavy metal pollution indices and statistical approaches for sustainable management. Environ. Chall. 5, 100230. https://doi.org/10.1016/j.envc.2021.100230.

Li, K., Yang, Q., Li, X., 2024. An analysis of the spatiotemporal variability of key water quality parameters in China. Article 9. Hydrology 11 (9). https://doi.org/10.3390/hydrology11090135.

Li, Y., Wang, M., Chen, X., Cui, S., Hofstra, N., Kroeze, C., Ma, L., Xu, W., Zhang, Q., Zhang, F., Strokal, M., 2022. Multi-pollutant assessment of river pollution from livestock production worldwide. Water Res. 209, 117906. https://doi.org/10.1016/j.watres.2021.117906.

Liu, X., Zhang, G., Sun, G., Wu, Y., Chen, Y., 2019. Assessment of lake water quality and eutrophication risk in an agricultural irrigation area: a case study of the chagan lake in northeast China. Water 11 (11), 2380. https://doi.org/10.3390/w11112380.

Magesh, N.S., Krishnakumar, S., Chandrasekar, N., Soundranayagam, J.P., 2013. Groundwater quality assessment using WQI and GIS techniques, dindigul district, tamil nadu, India. Arab. J. Geosci. 6 (11), 4179–4189. https://doi.org/10.1007/s12517-012-0673-8.

Matta, G., Srivastava, S., Pandey, R.R., Saini, K.K., 2017. Assessment of physicochemical characteristics of ganga canal water quality in Uttarakhand. Environ. Dev. Sustain. 19 (2), 419–431. https://doi.org/10.1007/s10668-015-9735-x.

Moeinzadeh, H., Yong, K.-T., Withana, A., 2024. A critical analysis of parameter choices in water quality assessment. Water Res. 258, 121777. https://doi.org/10.1016/j.watres.2024.121777.

Moto, E., Hossein, M., Bakari, R., Mateso, A.S., Selemani, J.R., Nkrumah, S., Ripanda, A., Rwiza, M.J., Nyanza, E.C., Machunda, R.L., 2024. Ecological consequences of microplastic pollution in sub-Saharan Africa aquatic ecosystems: an implication to environmental health. HydroResearch 7, 39–54. https://doi.org/10.1016/j.hydres.2023.11.003.

Nair, H.C., Joseph, A., Padmakumari Gopinathan, V., 2020. Hydrochemistry of tropical springs using multivariate statistical analysis in ithikkara and kallada river basins, kerala, India. Sustain. Water Resour. Manag. 6 (1), 9. https://doi.org/10.1007/s40899-020-00363-1.

Nayek, S., Choudhury, I., Roy, S., 2017. Water quality assessment of two constructed lakes (aritar lake & chaya taal lake) in sikkim during winter & summer season. Int. J. Adv. Res. 5 (7), 1411–1417. https://doi.org/10.21474/ijar01/4853.

Ndiaye, P.M., Bodian, A., Dezetter, A., Ogilvie, A., Goudiaby, O., 2024. Sensitivity of global hydrological models to potential evapotranspiration estimation methods in the Senegal river basin (West Africa). J. Hydrol. Reg. Stud. 53, 101823.

Niang, G., Sy, A.A., Faye, M., Faye, G., Ndiaye, A., 2022. Etude de l'érosion dans le bassin versant du lac de guiers. Nord du SéN.égal.

Niang, S., Gaye, A., Soda, M., Bouchez, A., Bouvy, M., Monet, G., Montuelle, B., 2017. Note sur la Qual. é Physicochim. du lac De. Guiers.

Ogilvie, A., Fall, C.S., Bodian, A., Martin, D., Bruckmann, L., Dia, D., Poussin, J.C., 2025. Surface water and flood-based agricultural systems: mapping and modelling long-term variability in the Senegal river floodplain. Agric. Water Manag. 308, 109254.

OLAC. (2013). *Rapport d'étude d'évaluation de la qualité des eaux du lac de Guiers* (p. 42).

OLAC, 2016. Situation de référence de la qualité de l'eau du lac de guiersRapp. D. éfinitive([Rapport final])80.

OLAC. (2021). Rapport d'étude de faisabilité sur le projet de renforcement de la résilience des écosystèmes du Ferlo au Sénégal (PREFERLO) – Vol. II: Rapport principal (mars 2021).

Onu, M.A., Ayeleru, O.O., Oboirien, B., Olubambi, P.A., 2023. Challenges of wastewater generation and management in sub-Saharan Africa: a review. Environ. Chall. 11, 100686. https://doi.org/10.1016/j.envc.2023.100686.

Ouma, K., Shane, A., Syampungani, S., 2022. Aquatic ecological risk of Heavy-Metal pollution associated with degraded mining landscapes of the Southern Africa river basins: a review. Minerals 12 (2), 225. https://doi.org/10.3390/min12020225.

Palviainen, M., Laurén, A., Launiainen, S., Piirainen, S., 2016. Predicting the export and concentrations of organic carbon, nitrogen and phosphorus in boreal lakes by catchment characteristics and land use: a practical approach. Ambio 45 (8), 933–945. https://doi.org/10.1007/s13280-016-0789-2.

Piper, A.M., 1944. A graphic procedure in the geochemical interpretation of water-analyses. Eos Trans. Am. Geophys. Union 25, 914–928. https://doi.org/10.1029/TR025i006p00914.

Razmkhah, H., Abrishamchi, A., Torkian, A., 2010. Evaluation of spatial and temporal variation in water quality by pattern recognition techniques: a case study on jajrood river (Tehran, Iran). J. Environ. Manag. 91 (4), 852–860. https://doi.org/10.1016/j.jenvman.2009.11.001.

Ren, X., Yu, R., Kang, J., Li, X., Wang, R., Zhuang, S., Wang, D., Zhang, X., 2022. Hydrochemical evaluation of water quality and its influencing factors in a closed inland lake basin of Northern China. Front. Ecol. Evol. 10, 1005289. https://doi.org/10.3389/fevo.2022.1005289.

Saleem, M., Jeelani, G., Shah, R.A., 2015. Hydrogeochemistry of dal lake and the potential for present, future management by using facies, ionic ratios, and statistical analysis. Environ. Earth Sci. 74 (4), 3301–3313. https://doi.org/10.1007/s12665-015-4361-3.

Sane, S., Ngansoumana, B., Samb, P., Noba, K., Arfi, R., 2015. Moteurs et conséquences de la resuspension dans un lac sahélien peu profond: le lac de guiers au Sénégal. Int. J. Biol. Chem. Sci. 9 (2), 927. https://doi.org/10.4314/ijbcs.v9i2.30.

Sani, Z., Katshiatshia, H.M., M. Tshimanga, R., Basamba, T.A., Odume, O.N., 2024. Relationship between land use and water quality in a tropical urban catchment of the Congo basin: a case study of N'Djili river catchment. Water Pract. Technol. 19 (4), 1272–1289. https://doi.org/10.2166/wpt.2024.080.

Sishu, F.K., Melese, T.B., Aklog, D., 2024. Assessment of heavy metal and other chemical pollution in lake tana along urban peripheries, Ethiopia. Water Pract. Technol. 19 (4), 1200–1218. https://doi.org/10.2166/wpt.2024.083.

Søndergaard, M., Larsen, S.E., Jørgensen, T.B., Jeppesen, E., 2011. Using chlorophyll a and Cyanobacteria in the ecological classification of lakes. Ecol. Indic. 11 (5), 1403–1412. https://doi.org/10.1016/j.ecolind.2011.03.002.

Taşdelen, S., 2021. Hydrogeochemical characteristics of spring waters for irrigation, Gokpınar basin case, denizli, Turkey. J. Agric. Sci. 27 (4), 516–525. https://doi.org/10.15832/ankut bd. 744844.

Tokatlı, C., Ustaoğlu, F., Muhammad, S., et al., 2024. Spatiotemporal variations, source identification, and risk assessment of potentially toxic elements in the surface water of felent stream impacted by the silver mine. Environ. Monit. Assess. 196, 870. https://doi.org/10.1007/s10661-024-13013-2.

USEPA. (2022). National recommended water quality criteria – aquatic life criteria [Online]. Washington, DC. [Data and Tools]. 〈https://www.epa.gov/wqc/national-recommended-water-quality-criteria-aquatic-life-criteria-table〉.

Ushurhe, O., Ozabor, F., Onyeayana, W.V., Adekunle, O., Christabel, I.C., Chike, D.F., 2024. Seasonal sodium percentage (%NA), ab sorption ratio (Sar) and irrigation water quality index (IWQI) determination for irrigation purposes along river ethiope, Southern Nigeria. Jo. urnal Water Re Source Prot. 16, 523–537. https://doi.org/10.4236/jwarp.2024.167029.

Varis, O., Fraboulet-Jussila, S., 2002. Water resources development in the lower Senegal river basin: conflicting interests, environmental concerns and policy options. Int. J. Water Resour. Dev. 18 (2), 245–260. https://doi.org/10.1080/07900620220135085.

Vasistha, P., Ganguly, R., 2024. Water quality characterization for two lakes in panchkula, haryana, India. Water Qual. Res. J. 59 (4), 268–293. https://doi.org/10.2166/wqrj.2024.124.

Visco, G., Campanella, L., Nobili, V., 2005. Organic carbons and TOC in waters: an overview of the international norm for its measurements. Microchem. J. 79 (1), 185–191. https://doi.org/10.1016/j.microc.2004.10.018.

Wang, H., Wang, T., Zhang, B., Li, F., Toure, B., Omosa, I.B., Chiramba, T., Abdel-Monem, M., Pradhan, M., 2014. Water and wastewater treatment in Africa – current practices and challenges. CLEAN Soil Air Water 42 (8), 1029–1035. https://doi.org/10.1002/clen.201300208.

WHO, 2017. Guidelines for drinking-water qualityWorld Health OrganizationGeneva, Switzerland〈https://iris.who.int/bitstream/handle/10665/254636/9789241550017-eng.pdf〉.

Wilcox, L.V., 1955. Classification and Use of Irrigation Water. US Department of Agriculture, Circular, Washington DC, p. 969.

Woldeab, B., Ambelu, A., Mereta, S.T., Beyene, A., 2019. Effect of watershed land use on tributaries' water quality in the east African highland. Environ. Monit. Assess. 191 (1), 36. https://doi.org/10.1007/s10661-018-7176-3.

Woolway, R.I., Kraemer, B.M., Lenters, J.D., Merchant, C.J., O'Reilly, C.M., Sharma, S., 2020. Global lake responses to climate change. Nat. Rev. Earth Environ. 1 (8), 388–403. https://doi.org/10.1038/s43017-020-0067-5.

World Bank, 2022. *Senegal Water Security : Executive Summary (English)*. World Bank Group, Washington, D.C. http://documents.worldbank.org/curated/en/099625203082232347.

Wu, B., Dai, S., Wen, X., Qian, C., Luo, F., Xu, J., Wang, X., Li, Y., Xi, Y., 2022. Chlorophyll-nutrient relationship changes with lake type, season and small-bodied zooplankton in a set of subtropical shallow lakes. Ecol. Indic. 135, 108571. https://doi.org/10.1016/j.ecolind.2022.108571.

Xiao, L., Zhang, Q., Niu, C., Wang, H., 2020. Spatiotemporal patterns in river water quality and pollution source apportionment in the arid beichuan river basin of northwestern China using positive matrix factorization receptor modeling techniques. Article 14. Int. J. Environ. Res. Public Health 17 (14). https://doi.org/10.3390/ijerph17145015.

Yuksel, B., Ustaoglu, F., Arica, E., 2021. Impacts of a garbage disposal facility on the water quality of Çavuşlu stream in giresun, Turkey: a health risk assessment study by a validated ICP-MS assay. Aquat. Sci. Eng. 36 (4), 181–192. https://doi.org/10.26650/ASE2020845246.

Zhang, X., Fang, C., Wang, Y., Lou, X., Su, Y., Huang, D., 2022. Review of effects of dam construction on the ecosystems of river estuary and nearby marine areas. Sustainability 14 (10), 5974. https://doi.org/10.3390/su14105974.